



Review

# Wireless Power Transfer in Electric Vehicles: A Review on Compensation Topologies, Coil Structures, and Safety Aspects

Benitto Albert Rayan<sup>1</sup>, Umashankar Subramaniam<sup>2,\*</sup>  and S. Balamurugan<sup>1,\*</sup> <sup>1</sup> Vellore Institute of Technology, Vellore 632014, India<sup>2</sup> Renewable Energy Lab, Department of Communications and Networks, College of Engineering, Prince Sultan University, Riyadh 11586, Saudi Arabia

\* Correspondence: usubramaniam@psu.edu.sa (U.S.); sbalamurugan@vit.ac.in (S.B.)

**Abstract:** The scarce availability of non-renewable sources and the staggering amount of pollution have inevitably provoked many countries to opt for renewable sources. Thence, invariably, more renewable energy-based applications are hoarded by market stakeholders. Compared to all spheres of renewable energy applications, a considerable part of the energy is pulled into transportation. Wireless power transfer techniques play a significant role in charging infrastructure, considering the current development and advancement in the automotive industry. It will promise to overcome the widely known drawbacks of wired charging in electric vehicles. The effectiveness of wireless charging depends on coil design, compensation techniques, and the airgap between the coils. However, coil misalignment, improper compensation topologies, and magnetic materials reduce the efficacy. We can improve efficacy by overcoming the problems mentioned above and optimizing charging distance, time, and battery size. This paper comprehensively discussed the various electric vehicle charging technologies in conjunction with common charging standards, a list of factors affecting the charging environment, and the significance of misalignment problems. Furthermore, this review paper has explored the suitable coil design structure and different compensation techniques for an efficient wireless charging network.

**Keywords:** charging; airgap; misalignment; wireless charging; compensation topologies; conductive charging; inductive charging; anti-misalignment



**Citation:** Rayan, B.A.; Subramaniam, U.; Balamurugan, S. Wireless Power Transfer in Electric Vehicles: A Review on Compensation Topologies, Coil Structures, and Safety Aspects. *Energies* **2023**, *16*, 3084. <https://doi.org/10.3390/en16073084>

Academic Editor: Mauro Feliziani

Received: 1 February 2023

Revised: 18 March 2023

Accepted: 21 March 2023

Published: 28 March 2023



**Copyright:** © 2023 by the authors. Licensee MDPI, Basel, Switzerland. This article is an open access article distributed under the terms and conditions of the Creative Commons Attribution (CC BY) license (<https://creativecommons.org/licenses/by/4.0/>).

## 1. Introduction

Electric Vehicles (EV) were invented in 1830 for moderate world transportation to replace Internal Combustion Engine (ICE) vehicles [1]. Some of the key benefits of EVs are: (a) negligible carbon emissions; (b) relatively higher efficiency; (c) less noise; and (d) low maintenance requirements compared to fossil fuel-based vehicles. Recharging the batteries in an EV is similar to refueling an ICE vehicle [2,3]. EV charging stations' infrastructure costs are less than fossil fuel-based vehicles' current refueling stations. It is also one reason to switch conventional transportation technologies to electrified ones [4,5].

Before the invention of electric vehicles, the Italian scholar Alessandro Volta was the first person to clinically invent that electrical power could be stored in a battery (with components such as copper-zinc plates separated by paper discs soaked in brine solution). This invention is prominent in EV applications, mostly as a primary power source and secondly as hybrid counterparts. Commonly, EVs contain three significant parts: a converter for charging, battery storage, and the type of motor used [6,7]. There are two significant domains of charging methods available in EVs. Those are conductive (plug-in) charging and wireless charging. Conductive or plug-in charging connects the EVs and charging stations with appropriate charging cables and ports. It takes less time to charge a battery, and Direct Current (DC) power can be shared directly with the battery. There are some constraints to the conductive charging method. The constraints are the time taken to

connect the charger; EVs must be standing within the charging cable length; potential traffic congestion; and the limited number of charging stations [8]. Electric charging stations can be placed only at selected places. Since most of these charging stations require high-power transmission and the corresponding accessories (to decrease the charging time for each vehicle), more precautions have to be taken when charging a battery. The drawbacks of conductive charging can be overcome by using alternative charging methods like wireless power transfer. Furthermore, many researchers have contributed to improving and upgrading the efficacy of electric vehicles by minimizing the charging time and creating a better battery management system [9]. Nevertheless, batteries remain the primary source of these EVs. Depending on the usage and the charge level, an electric vehicle's battery pack must be recharged at stated intervals. Faraday invented the electric motor and the electromagnetic induction principle for electromagnetism in 1821 and 1831, respectively.

Based on Faraday's laws of electromagnetic induction, power can be transferred from one place to another without using a wire. In 1859, lead-acid batteries were invented in Belgium and incorporated into a tricycle in France and the United States of America (USA). The basic knowledge of wireless power transfer (WPT) was developed by Nikola Tesla, who did his experiment using the Wardencliff Tower to transfer electrical energy without wires around the world in late 1910 [10]. Although his experiment was abandoned later, his idea of wireless power transmission has been far-reaching to date. WPT methods are separated into two types on the basis of vehicle movement. Firstly, the simplest WPT method is static wireless charging. Static charging is implemented when the EV is in a stand-alone condition. Secondly, the dynamic wireless charging method allows wireless charging to be achieved when vehicles are in a mobile state with the help of a proper control strategy and speed limitations [11,12]. These two methods come under the category of inductive power transfer.

The inductive power transfer efficiency can be improved in different ways. The structure of transmitter and receiver coils [13], the alignment between the coils, the selection of suitable batteries and proper charging standards, and shielding for the electromagnetic field like aluminum shielding around the transmitter and receiver pads are all important [10]. Several coil structures are upgraded daily with the help of suitable simulation software (ANSYS and COMSOL). The misalignment problems may arise between two coils due to the human's fault or the placement of the coils. The anti-misalignment techniques help to overcome those problems through the use of some developed optimization algorithms (phase angle optimization and balanced particle swarm optimization) and sensor placement techniques. Based on these techniques, the efficiency of the wireless charging system can be improved.

EV charging is an emerging technology in transportation engineering. However, as technology advances, there is a greater need to address the power grid's demand problem. Vehicle to Grid (V2G) technology is one of the emerging technologies to solve the power demand problem. With V2G technology, EVs can deliver excess power to the power grid. H. Nguyen et al. have reviewed the V2G implementation in plug-in charging-based EVs [14]. Essential requirements for technology are flexible, automatic, bi-directional converters (in both charging and discharging). As per research, WPT can efficiently work on V2G technologies. Bi-directional converters can achieve charging in two ways, like Grid to Vehicle (G2V) [15,16] and V2G, which could eliminate energy loss in batteries while the vehicle is parked [17,18]. Therefore, renewable energy sources can efficiently be used in transportation and easily integrate with V2G technology instead of fossil fuels. Furthermore, due to advancements in automation, wireless charging can be very easily adopted with EVs. The comparison between wired and wireless charging-based EVs and the integrity of V2G is discussed in [19,20]. Wired and wireless charging can achieve integrity with 10% and 65% grid [21–24]. Wireless communication devices are mainly helpful in attaining the efficient V2G technique in EVs. If wireless charging and a power grid are integrated into a vehicle, excess energy can be used for required endometrial requirements [25–29].

Overall, this article discusses the various coil structures for wireless power transmission and their exclusivities. Additionally, this paper discusses the issues in wireless

power transmission systems, including power losses, coil misalignment, and safety. Various strategies, including switching losses reduction, frequency range estimation, and electrical and mechanical compensations, are reviewed and discussed in detail to enhance the power transmission performances. Further, the dynamic and quasi-dynamic charging problems are discussed, and the suitable anti-misalignment techniques are analyzed in detail. The review shows that the triple quadrature coil shapes with double-sided LCC and LCC—SS compensation and tripolar with S-shaped coils will significantly reduce misalignment and airgap issues. The various wireless power transmission systems are viewed and deliberated in detail from a techno-economic perspective.

This paper is organized into eight sections. The consolidated introduction of EVs and EV charging systems is confined to the previous passage. The following sections have discussed EV charging methods, wireless charging technologies and their classifications, different structures of a coil, and factors affecting the wireless charging infrastructure. Additionally, standard power levels of plug-in charging, comparisons between the various charging levels and battery capacities of current EVs, different compensation topologies of primary and secondary circuits, standards of wireless charging systems, and an economic analysis of WPT systems. The layout of the paper organization is shown in Figure 1.

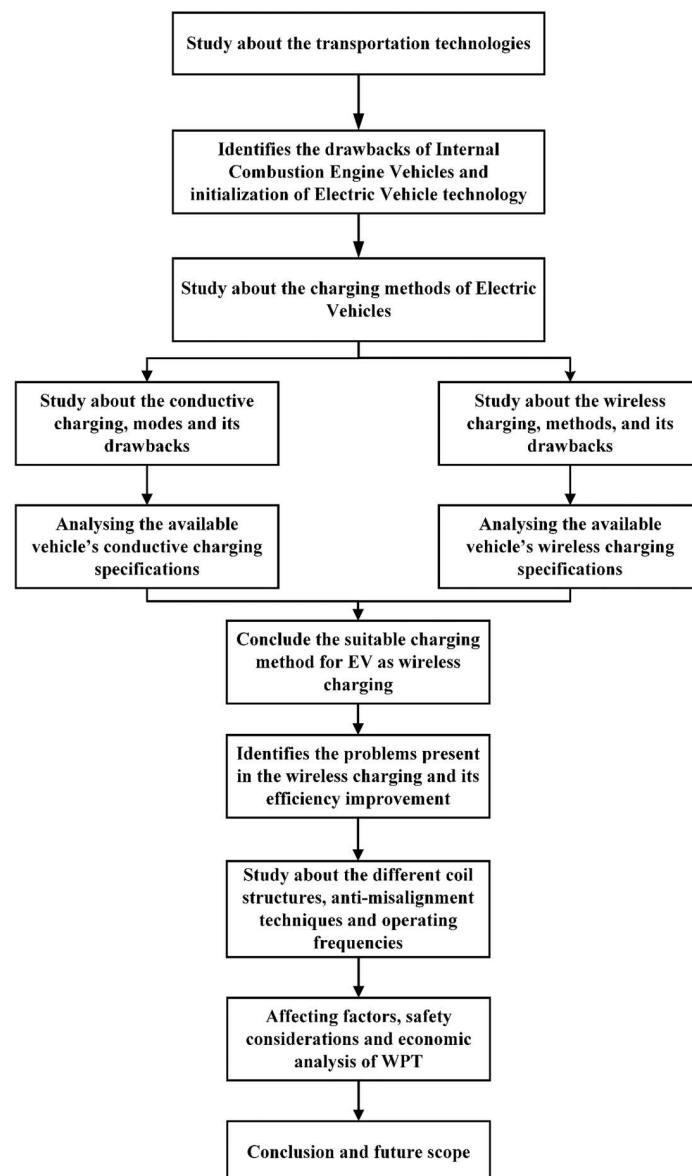


**Figure 1.** Layout of paper organization.

## 2. EV Charging Methods

Charging methods play an essential role in the improvement of EV mobility. The types of charging methods for EVs are shown in Figure 2. In addition, the basic classifications for EV charging are shown in Figure 2a. EV charging methods are primarily classified into two types [30–33]. They are conductive (plug-in) charging or wired charging, and wireless charging. Conventional EVs require more time to charge their batteries when compared to hybrid vehicles. In fast charging mode, EV batteries can charge up to 50% within 3 min and 80% within 15 min [34,35]. However, fast charging techniques reduce the battery pack’s life. Therefore, real-time customized, fast chargers are invented to overcome the demerits of slow chargers [36].

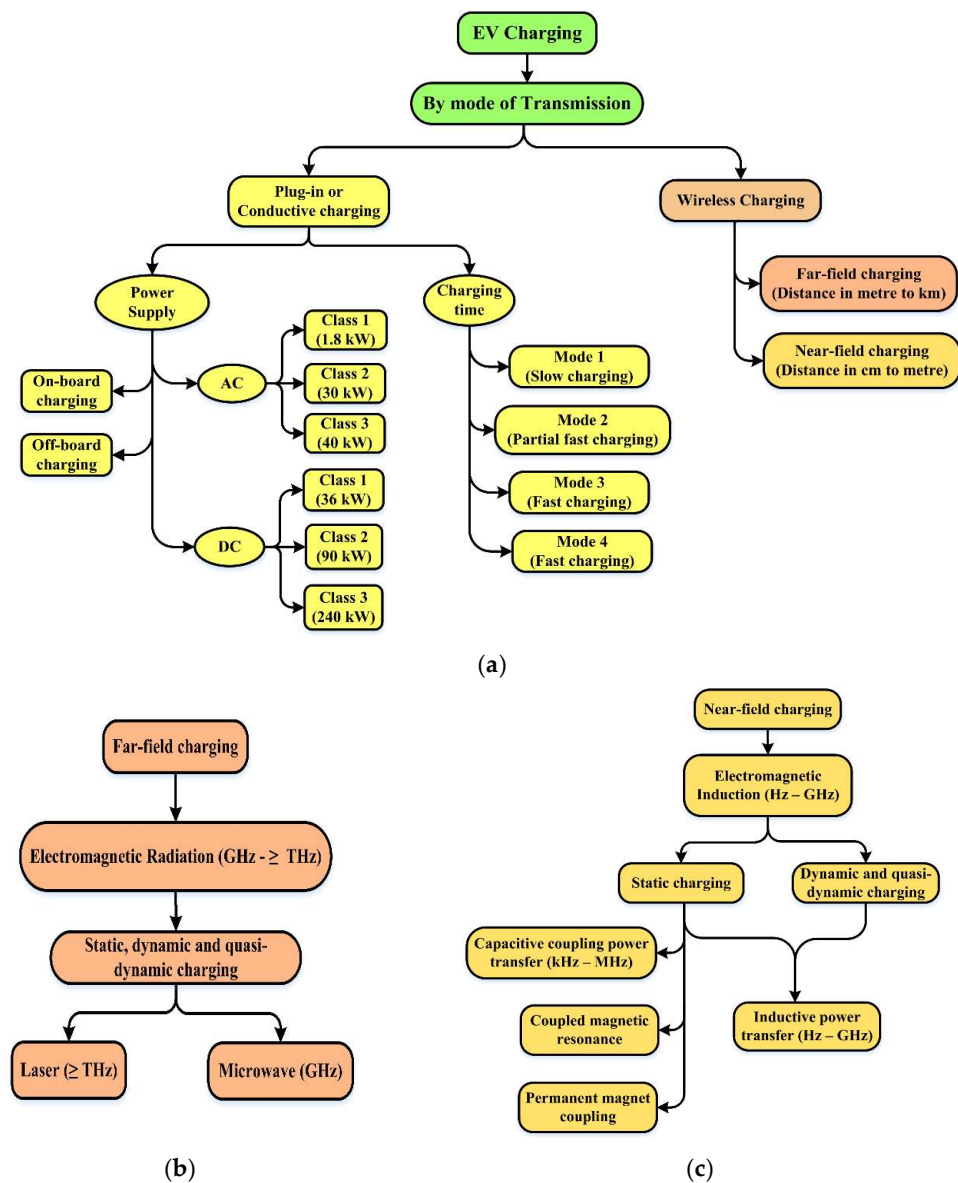


**Figure 2.** Schematic diagrams of charging types in EVs. (a) Classifications for charging EVs. (b) Types of far-field charging. (c) Types of near-field charging.

Battery swapping is also one of the alternate solutions for EV charging. It is also called a Battery Exchange System. In battery swapping, we can get the batteries by rental type from battery swapping stations monthly [24]. In the battery swapping technique, drivers do not need to wait to charge the vehicle before getting out of it. The V2G technique can be easily implemented using the returned batteries available at battery swapping

stations [24,26]. However, the battery swapping technique is more costly than the ICE engines' fuel cost. This technique needs expensive batteries; battery specifications will change from one vehicle to another, and the battery swapping station owners will fix their battery price [27].

### 2.1. Conductive Type, Plug-In Charging, or Wired Charging

The conductive or plug-in charger establishes the physical connection between the grid power source and the electric vehicle. This type of charging can be achieved with the help of proper values for the rectifier and converters and overall system efficiency based on those devices. There are two types of conductive charging methods. The first method is called on-board conductive charging with unidirectional and bidirectional converters. Rectifiers and battery current regulators are fixed inner surfaces of the EV. In the second method (called an off-board charger with unidirectional and bidirectional converters), battery current regulators and rectifiers are placed outside the EV.

Depending on the charging capacity of the batteries, there are two ways to charge the vehicle. They are normal or slow charging and fast charging [37]. In the normal charging method, an Alternating Current (AC) or DC power from a grid is rectified, boosted, and transferred to the electric vehicle through wires. In fast charging, an off-board charging device supplies rectified and controlled DC power that charges the vehicle battery pack [38]. Since the rectifier and charger hardware is off-board, charging the vehicle at higher charging rates is possible. Depending on the charging time and battery capacity level, there are four modes of charging technique. Mode 1 is the slowest charging, and it takes up to 8–10 h to charge the battery. Mode 2 is a partial fast charge. These two charging modes apply to a single-phase AC power supply [39]. Usually, Mode 1 and Mode 2 charging methods are suitable for domestic and industrial places. Mode 3 and Mode 4 are fast charging techniques using a three-phase supply of both AC and DC. Within half an hour, the battery will get a full charge. Charging methods are divided into three classes based on the power supply level, each with AC and DC supplies [38]. The time duration of charging will vary between AC and DC power levels. Classes of power levels in EV charging are shown in Table 1.

**Table 1.** Classes of power levels in EV charging.

S. No	Supply and Class	Voltage (V)	Phase	Current (A)	Power Level (kW)	Mode of Charging
1	AC Class 1	120	1	12, 16	1.6, 1.8	Normal [8,39]
2	AC Class 2	240	1	80	Up to 30	Fast [8,40]
3	AC Class 3	240 and 415	1 and 3	100	20–40	Normal and Fast [8]
4	DC Class 1	200–450	DC	80	36	Fast [8,39]
5	DC Class 2	200–450	DC	200	90	Fast [8,39,40]
6	DC Class 3	200–600	DC	400	240	Fast [39,40]

For safety purposes, EV users must use isolation topologies if the input supply voltage is less than 25 V or more than 60 V. Isolation topologies are hard- and soft-switching topologies. They are switching-based methods that can operate the switches by turning on and off conditions with the relationship between the voltage and current. Hard switching helps to turn on and turn off the transistor switch by adding voltage or current to change the states from collector to emitter or emitter to collector [38,39]. Using this technique, electromagnetic interference happens as a by-product. The schematic representation of EV isolated hard switching is presented in Figure 3. This isolation topology produces more stress on electronic switches for continued switching, which is heavy switching for electronic components. The main drawback of this topology is that it introduces more

switching loss. This type of switching is used in simple switches, switch-mode power supplies, and motor drive inverters [2].

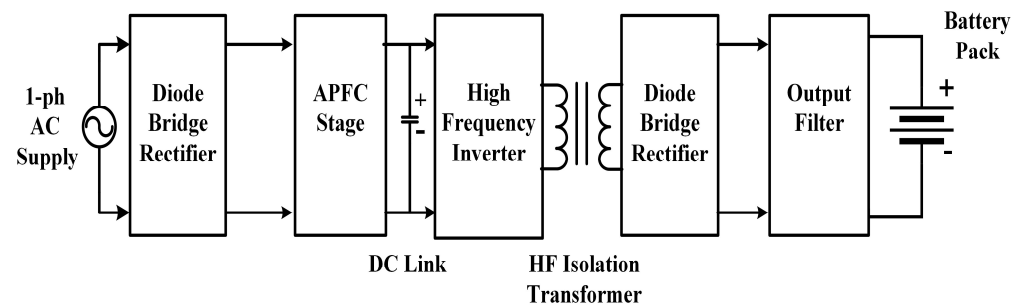


**Figure 3.** EV isolated hard switching topology.

The EV isolated soft switching topology shown in Figure 4 works under the principle of electric resonance. It can operate at Zero Voltage Switching (ZVS) and Zero Current Switching (ZCS), which can reduce Electromagnetic Interference (EMI) issues at the source level in the design. Soft switching is used to turn on and off the switches by using the LC (Inductor Capacitor) resonant circuit to produce the forced swing on switches. This topology needs complex control circuits. However, it suffers from fewer switching losses, thereby increasing operating efficiency. Furthermore, reduced switching losses can be designed for higher operating frequencies, making the design more power-dense [2].

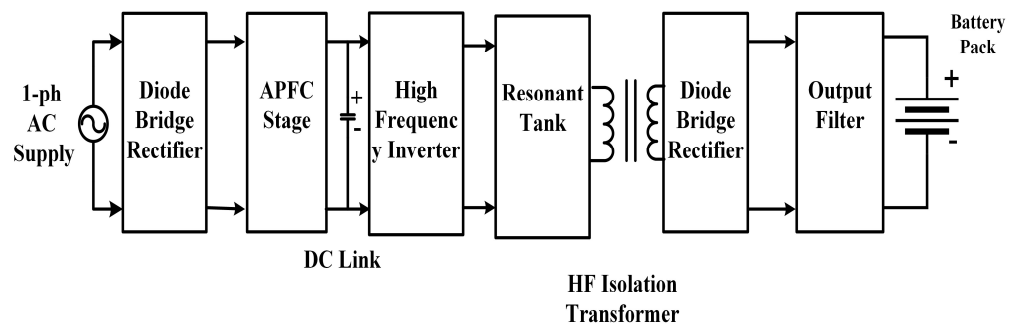


**Figure 4.** EV isolated soft switching topology.

When compared to hard switching, soft switching has an added advantage in the safest operating zones. Exploiting these techniques, various companies implemented several EVs and Plug-in Hybrid Electric Vehicles (PHEVs) with different charging classes, battery capacities, and home appliances like induction cooktops, microwave ovens, and induction rice cookers. Table 2 shows the various charging levels and battery capacities of EVs and PHEVs. Based on the available feedback, some advantages are present in conductive charging [41,42].

**Table 2.** Various charging levels and battery capacities of EVs.

Model	Charging Duration (Hr)	Battery Capacity (kWh)	Class of Charging	Charging Duration (h)	References
Porsche Panamera SE—Hybrid (PHEV)	10	9	Class 1/Class 2	10/2.5	[43]
Audi A3 e-tron (PHEV)	11	9	Class 1/Class 2	8/2.5	[44]
Cadillac ELR (PHEV)	11	16.5	Class 1/Class 2	12.5–18/5	[45]
Chevy Spark (Pure EV)	11	19.44	Class 1/Class 2/ DC Fast	20/7/20 min	[46]
Chevy Volt (PHEV)	11	18.4	Class 1/Class 2	13/4.5	[46]

Table 2. Cont.

Model	Charging Duration (Hr)	Battery Capacity (kWh)	Class of Charging	Charging Duration (h)	References
Ford C-Max Energi (PHEV)	11	7.6	Class 2	2.5	[47]
Mercedes S550 Plug-in Hybrid	11	8	Class 1/Class 2	2/4–5	[48]
Mercedes C350 Plug-in Hybrid (PHEV)	11	6.2	Class 2	2	[49]
Smart Electric Drive (Pure EV)	11	17	Class 2	2.5	[50]
Toyota Prius Plug-in (PHEV)	11	9	Class 1/Class 2	5.5/2	[51]
Mitsubishi i-MiEV (Pure EV)	11	16	Class 2/Class 3	6, 8, 10/30 min	[52]
Nissan LEAF (Pure EV)	11/22	24	Class 1/ Class 2/Class 3	22, 8, 30 min	[53]
Porsche Cayenne S E-Hybrid (PHEV)	12/24	11	Class 2	3/90 min	[54]
Volkswagen e Golf (Pure EV)	12/24	36.6	Class 1/Class 2/ DC Fast	24/9/30 min	[55]
Ford Focus Electric (EV)	22	23	Class 1/Class 2	20/3–4	[56]
Fiat 500e (Pure EV)	22	24	Class 2	4	[57]
Kia Soul (Pure EV)	22	27	Class 1/ Class 2/Class 3	24/4–5/43 min	[58]
Honda Accord Plug-in Hybrid (PHEV)	22	7	Class 2	3	[58]
Honda Clarity Electric (Pure EV)	25	25	Class 1, Class 2, and DC Fast	19, 3 h and 30 min	[59]
BMW i3 (Pure EV)	25	24	Class 1, Class 2, and DC Fast	22, 8, 30 min	[60]
Mercedes B—Class Electric (Pure EV)	29	28	Class 2	2	[61]
Tesla Model S (Pure EV)	29/58/255	85	Class 1/Class 2/ Super Charger		[62]

Most EVs use lithium batteries (replacement of the batteries is required) or lithium-ion batteries (recharging of the batteries is required) [63–65]. They must be maintained at proper charging and discharging levels with appropriate control strategies for a safe and efficient perspective.

## 2.2. Wireless Charging System

Conductive or plug-in charging is more efficient and requires less time for charging. Despite this convenience and flexibility, more research is needed on wireless charging technologies to overcome the defects of plug-in charging technology. Wireless power transmission is also called cordless power transmission, and inches to kilometers of distance can be quickly achieved [61]. This type of power transmission can be made by using a microwave, radio wave, electromagnetic field, or electrostatic effect as a transmission medium. Recently, many companies equipped their products with wireless charging features, like mobile phones, laptops, watches, and toothbrushes [66]. Many research and development projects aim to improve the efficiency and distance between the transceiver and receiver coil in meters using suitable electronic circuits and proper compensation networks. After the advancement of wireless charging technology, it is implemented in high-power applications like vehicles and industrial applications [2,67–70].

To achieve maximum efficiency, more attention is needed for EV batteries. They are the heart of the EV system. Several batteries and supercapacitors are available for the different energy storage applications in EVs. It can be chosen while aligning with various aspects like life cycle, efficiency rate, power-consuming capacity, cost, and safety. Supercapacitors are suitable for limited applications due to their limited withstand capacity and repeated charging [71–73]. So, batteries are used in EVs as a storage device; currently available batteries are Lithium-Ion (Li-Ion), Molten Salt (Na-NiCl<sub>2</sub>), Nickel Metal Hydride (Ni-MH), and Lithium Sulfur (Li-S). These battery performances are varied based on their characteristics and charging cycles [74].

Na-NiCl<sub>2</sub> batteries were implemented in 1946, and as per the survey results, this type of battery is suitable for EVs due to the energy consumption ratio (12.6 kWh/100 km). Moreover, it is low cost and can give a better performance during critical conditions. Less efficacy at higher operating temperatures is the notable drawback of this battery. This temperature may affect the internal parts of the battery, like the electrolytes, if the vehicle is in a standstill condition. So, it requires some other system accessories to maintain the proper operating temperature under nominal conditions [75].

Li-S batteries can also maintain a high level of energy consumption of 17.2 kWh/100 km and were invented in 1960. These batteries have a low weight, a lower cost, and higher energy storage levels than other battery technologies. So, it can be suggested for relatively high-power applications. Ni-MH batteries also maintained a power consumption level of 15.7 kWh/100 km and were invented in 1967. However, the weight, energy density, and battery price are too high. So, it is not suitable for higher power applications.

At present, most automobile companies are employing Li-Ion batteries for their EVs. Li-Ion batteries have an energy consumption of 14.7 kWh/100 km at a low price [75–78]. It has updated battery technology, a higher energy storage capability, an improved life cycle, and is lighter. It needs protection with some safety arrangements over thermal exposure [63,79–82]. A lot of research is being done to extend the life of Li-Ion batteries by swapping the materials used for the anode and cathode. The anode of a typical Li-Ion battery is made of graphite. Modifying the cathode material will enhance the Li-Ion batteries' performance and security features. Several possible combinations include lithium-cobalt oxide, lithium-manganese oxide, lithium nickel-manganese-cobalt oxide, lithium nickel-cobalt-aluminum oxide, and lithium-iron phosphate. The EV manufacturers suggest lithium nickel-manganese cobalt oxide to enhance the Li-Ion batteries effectiveness and safety features [83]. The comparison between the different EV battery specifications is shown in Table 3.

**Table 3.** Comparison between the EV battery specifications [63,82].

Specification	Type of Battery			
	Li-Ion	Na-NiCl <sub>2</sub>	Ni-MH	Li-S
Charge capacity (Ah)	75	84	85	80
Voltage (V)	323	289	288	305
Energy (kWh)	24.2	24.2	24.2	24.2
Total cell row	17	30	20	1
Operating Temperature (°C)	33	270	36	30
Weight (kg)	318	457	534	173
Price of Battery (EUR)	300	500	400	250

The health of the battery can be estimated using battery management techniques. The State of Charge (SOC) and State of Health (SOH) estimation methods can improve the



battery's reliability, life cycle, and efficiency. In addition, other battery management system methods are available for estimating SOC and SOH [84–89].

### 3. Wireless Charging Technologies

WPT is divided into far-field and near-field WPT techniques based on the transferring distance of inducing power. Further, these two WPT systems are classified into six types based on the employed transferring medium. Far-field charging types are microwave and laser, and near-field charging types Capacitive Coupling Wireless Power Transfer (CCWPT), Coupled Magnetic Resonance (CMR), Inductive Power Transfer (IPT), and Permanent Magnet Coupled transfer (PMC). Microwave and laser technologies fall under the category of far-field wireless technology, whereas IPT, CMR, and PMC come under the category of near-field wireless technology. Based on the vehicles' mobility state, WPT is classified into two methods. The first method is static WPT while the vehicle is in a stand-alone state [36,66–70,90–93] and the second method is dynamic WPT when the vehicle is in a mobile condition [12,36,69,70,94–96]. Each method of WPT is important for different applications. As a result, it is challenging to propose an efficient method for a particular application. CMR is more suitable for lower-power applications, whereas IPT is more suitable for high-power applications without any resonant circuit. WPT techniques can achieve 85–96% efficiency with less airgap between the primary and secondary coils. If the airgap increases, then the power flow efficiency automatically decreases. More research is going on to improve efficiency by increasing the airgap distance of the transmitter and receiver coils [62]. More attention is needed to maintain the proper efficiency in a large airgap concerning the magnetic coupling coefficient. If the magnetic coupling coefficient values are high, it is possible to achieve valuable efficiency, greater than 90% [67–69].

#### 3.1. Far-Field Charging

In far-field WPT, power can be transmitted from meters to kilometers. The types of far-field charging with respect to frequency levels are shown in Figure 2b. There are three significant processes available in far-field WPT. First, the process initiates by converting the electrical energy into a radio wave or laser beam. Next is the spatial transmission of the converted radio wave or laser beam. Finally, the collection of all radio waves at a destination and conversion into electrical energy [88]. Using proper transmission and receiver mediums, this type of power transfer mechanism is easily achieved. Based on the transmission frequency, two types of far-field WPT technologies are currently available. They are microwave or radio waves [5,97–101] and laser beams [102–105].

##### 3.1.1. Microwave Power Transmission

The modern improvement in wireless power transmission is microwave power transmission. Microwaves have been operating in domestic applications since 1960. In 1964, William C. Brown experimented with powering a helicopter using microwave transmission and a “rectenna”, which converts microwaves into DC. In the early 1980s, National Aeronautics and Space Administration (NASA) scientists developed a thin-film plastic rectenna using Printed Circuit Board (PCB) technology that weighed less than one-tenth as much as the state-of-the-art rectenna. This advancement led to the improvement of the Stationary High-Altitude Relay Platform (SHARP) technology used to develop uncrewed aircraft using microwave-based power transmission [5]. Microwave-based power transmission is the most suitable method for long-distance power transfer [97]. This power transmission was introduced in 1968 in the USA. However, microwave power transmission uses a higher range of frequency bandwidth (in GHz) during transmission. This transmission type can only be implemented in non-human habitats like forests or deserts (the best-case scenario is zero terrestrial habitats) [94]. The working of satellites is based on microwave power transmission, where solar energy is converted into electricity in space and then transmitted back to the earth as a microwave. Further, microwaves can easily be affected by changes in

seasonal parameters and moisture contents available in the air. Additionally, microwaves are challenging to pass through solid objects [99–101].

### 3.1.2. Laser Power Transmission

Laser technology transfers the energy over the required distance with lower efficiency. It is not suitable for EV charging. Moreover, the power transfer mechanism using a laser is also intricate. In laser technology, power should be transferred as a high-frequency laser beam. Its work is based on the photoelectric effect (as proved in 1965) [102]. So, it is mandatory to convert the electrical energy into a high-frequency laser beam using power over fiber technology and deliver it to the photovoltaic cell. This type of transferring mechanism is termed power beaming. The electromagnetic radiation spectrum of lasers is from 180 nanometers to 400 nanometers. It is closer to the value of the visible-region spectrum.

For this reason, the laser beam must be concentrated on the photovoltaic cell. With the help of power converters again, electrical energy can be transformed [103]. Laser's transmission is a flexible process applicable for mobile applications with a kilometer-long power transmission range. However, more precautions must be taken with laser technology. The maximum efficiency ranges between 20% and 30% on the receiver side. The laser beam's directionality problems could affect the human body's electro-chemical mechanism [104–107].

## 3.2. Near-Field Charging

Near-field power transmission states that the electrical power transmission is within a small region, and hence there is no need for a high-frequency range of conversion and conversion medium [108]. The range of the airgap between the primary and secondary coils is remarkably smaller in near-field WPT. It is in the millimeter-to-meter range. The classifications for near-field charging are shown in Figure 2c. Near-field WPT efficiency is based on the transmitter and receiver modules' size, material, and shape. The electric power can be shared with the help of an electromagnetic field by using proper electrodes and magnetic fields through coils. It is possible to transfer the power in two ways: (i) by electric field WPT and (ii) by magnetic field WPT. Power can be transmitted with minimal distance in the electric field because of the high decay rate. On the other hand, there are chances for delivery power reduction due to the increased airgap between the primary and secondary coils. Power can be transmitted over a longer distance in the magnetic field compared to the electric field WPT [109].

### 3.2.1. Capacitive Coupling Wireless Power Transfer

CCWPT is an essential and efficient type of WPT technique. This power transmission can be achieved by using metal electrodes with the help of capacitive coupling. Non-radiative electric fields share the electrodes, i.e., the power transmission is limited to the shortest distance. The equivalent circuit of CCWPT is shown in Figure 5.

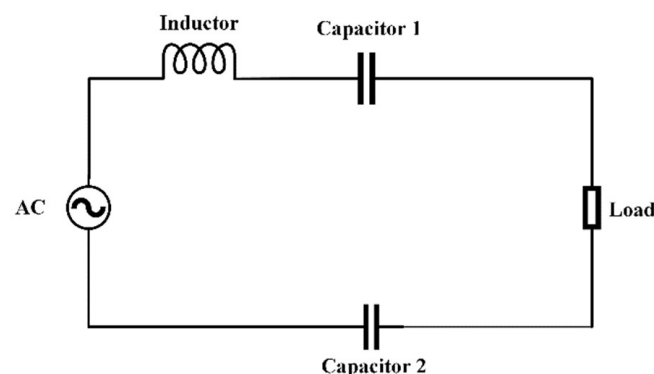


Figure 5. Equivalent circuit of CCWPT.

The transmitter can release the electric field to a suitable receiver or absorbing material if the electric transmission field-domain reduces, i.e., when the distance between the two electrodes decreases. The output voltage from Figure 5 is formulated as:

$$V_{OUT} = \frac{V_{IN}}{j\omega L + \frac{2}{j\omega C_{cc}} + R_L} R_L \quad (1)$$

From the above equation, the system's output voltage can be increased in three ways. The initial method is to increase the operating frequency and reduce the impedance of the model. The next method is compensation, which can also restrict the capacitive impedance. The last method is to improve the voltage by using boost-up circuits. Less cost, weightlessness, and low eddy current loss are the notable merits of this method [110]. However, CCWPT technology can only be applicable to low-powered applications [111] and smaller airgap systems like biomedical equipment [112,113], mobile devices, and Light Emitting Diode (LED) lighting [114,115]. Liang et al. developed a high-power dynamic capacitive power transfer system for railway applications with a power of 3 kW and a 92.46% efficiency. High-power transmission needs to concentrate more on high-voltage stress issues [1,115,116].

### 3.2.2. Coupled Magnetic Resonance Charging

Coupled magnetic resonance-based wireless charging works based on the coupling theory mode and allows power to transfer over the desired distance. This type of charging uses two antennas that connect the primary and secondary parts at the same operating frequency levels. This charging system works in the MHz range of frequency levels. Many research industries and institutes work on magnetic resonance and electric resonance couplings, like Nagano Japan Radio Co., Ltd. and Toyohashi University of Technology. Massachusetts Institute of Technology, Cambridge, MA, USA, developed magnetic resonance type charging [117]. It consists of primary and secondary coils, compensating capacitors for power factor correction, and developing a resonant condition for maximum power tracking. Online Electric Vehicle was implemented in South Korea based on resonance coupling using Dynamic Wireless Charging (DWC) [118–120]. In a dynamic WPT system, achieving an efficiency of 90% at a range of 1 m [4,121] is possible. The efficiency can be improved by using magneto plate wires [122].

### 3.2.3. Permanent Magnet Coupling Charging

The University of British Columbia implemented a permanent magnet coupling-based WPT technique with neodymium permanent magnets that act as a magnetic coupler and work based on the magnetic gear effect principle. Magnetized primary and secondary side rotors rotate with equal speed. This rotation speed is called synchronous speed. Some drawbacks of this type of charging are the noise, vibrations, and temperature produced by many mechanical elements. In particular, alignment and maintenance are notable drawbacks of the permanent magnet WPT technique. Compared to other technologies of EV charging, permanent magnet WPT is not convenient due to its bulky size, lower efficiency, rotating mechanical parts, etc. [123]. Covic et al., developed a permanent magnet WPT model with a 150 mm airgap and 81% efficiency at a frequency of 150 Hz [124,125].

### 3.2.4. Inductive Power Transfer

Inductive power transfer works based on electromagnetic induction within airgaps, as discussed in [7,126–128]. However, Lenz's law and Faraday's law are the key principles for the inductive type of power sharing. According to the law, time-varying current passes through a conductor (transmitter), producing an electromagnetic field around the conductor. Due to this, the secondary coil (receiver) receives electromotive force [129]. Then, the secondary coil is attached to the battery or load, and power is transferred throughout the circuit without any physical contact. Transmitting and receiving the electromotive

force can be achieved by using the proper magnetic materials [130]. Figure 6 shows an experimental block diagram of the inductive-based power transfer technique. Initially, Oersted introduced electromagnetism and electromagnetic field generation around the current-carrying conductor [131].

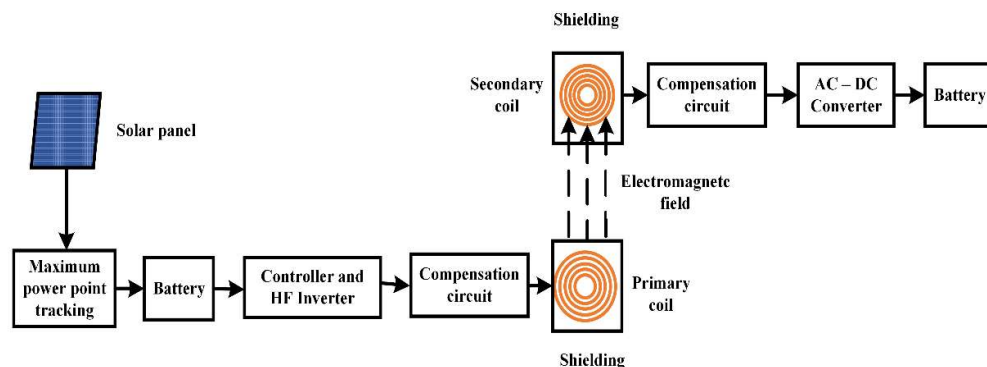


Figure 6. Block diagram of the inductive power transfer.

The theory and properties of the magnetic field are revealed by using Ampere's law, Faraday's law, and Biot–Savart's law [132,133]. In 1864, Maxwell's equation was implemented and presented, showing the relationship between the electric and magnetic fields [134]. In 1888, Hertz transmitted electrical power across the shortest airgap with the help of an oscillator and inductive coils [135]. In 1894, Leblanc and Hutin received a patent for introducing electric traction techniques in a vehicle using WPT [136,137]. Otto developed a WPT-based small trolley bus at the University of Auckland [138]. At the same time, the WPT project was implemented in the USA and Canada [139]. In 1982, Partner for Advanced Transit and Highways (PATH) completed a wireless charging project with 60% efficiency at 400 Hz frequency with a 50–100 mm airgap [140]. During 1990, IPT systems were implemented by Transport Urban Libre Individual Public (TULIP) in France and Wampfler Company in Germany. Showa Aircraft Company implemented their IPT system with a 14 cm airgap and an efficiency of 92% for 30 kW of power at a 22 kHz frequency [141]. In 1999, a new inductive coupler was implemented and achieved 97% efficiency at an output power of 8.3 kW with a 3 mm airgap between the primary and secondary coils [142]. For smaller WPT electronic objects, the Radio Frequency Identification (RFID) system can work efficiently [143,144]. IPT systems can be classified into non-resonant IPT and resonant IPT. The level of resonance during the operation remains the fundamental difference between these two methods. The non-resonant IPT method is efficient and well suited for small airgap power transfer applications. The resonant IPT method operates at the same frequency and is suitable for large airgap power transfer applications. Based on this technique, two EV applications are developed and explained in the upcoming sections.

### 3.2.5. Static Charging

Static charging systems work under a similar principle to IPT. This charging method can be implemented in vehicle parking areas, traffic signals, and toll plazas. Lukic and Pantic [36] described the present static wireless charging system and consolidated the improvement of industry-wide standard guidelines by the SAE [145]. Efficiency-wise, static wireless charging is more suitable for EVs. In static WPT, efficiency may be affected because of transmitter and receiver coil misalignment. It is possible to overcome this with mechanical and proper compensation technologies.

Many researchers contribute to eliminating the misalignment problems in static WPT [70,103]. Figure 7 shows the schematic diagram of the static WPT of EV. The system's efficacy can be improved by concentrating on each conversion stage. The whole block diagram is split into two stages. The initial stage consists of input power like a DC or AC source and a high-frequency inverter. If the input power is AC, it should be converted into DC with power factor correction and shared with the high-frequency inverter. Inductive

power transfer needs only AC power at a high frequency to achieve efficient power transfer. Solar or DC input power can be directly shared with the high-frequency inverter, as in the proposed system by the authors of [146,147]. Then an inverter converts the DC power into high-frequency AC power. We can achieve up to 97% efficiency using the above technique.

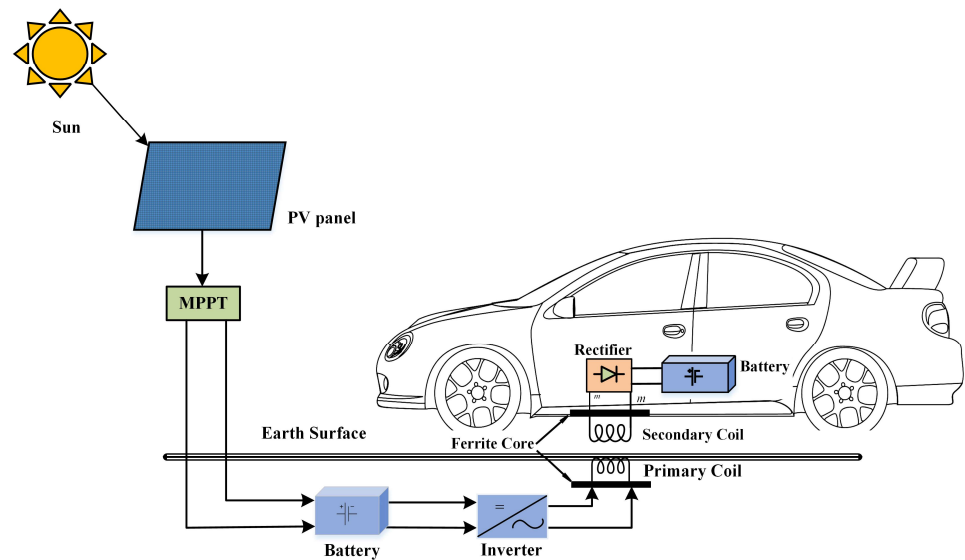


Figure 7. Schematic diagram of static WPT.

The final stage comprises inductive coils, compensation networks, and an AC-to-DC converter. After the high-frequency inverter's AC power is transferred to the primary coil, an electromagnetic field is produced around the primary coil based on Ampere's law. This electromagnetic field is produced by AC power in the receiver coil, which is placed at a limited distance from the transmitter coil based on Faraday's law of electromagnetism. Then, the AC power will be converted into DC power by using the converter and stored in the battery. In the final stage, we can get up to 95–97% efficiency. Since these two stages show high efficacy, it is possible to get a system efficiency of 85% or more. Many automobile companies are working on static wireless charging for EVs. Qualcomm and Oak Ridge National Laboratory (ORNL) have already launched their products at an efficiency of 95% or more with proper compensation topologies [148,149].

### 3.2.6. Dynamic Charging

A vehicle can be charged in the mobile state by using DWC. This type of charging reduces the buffer time for charging the vehicle. It was implemented in 1978 by Bolger [139]. DWC eliminates EV charging problems such as continuous power sharing, current-controlled inverters, and Electromotive Force (EMF) characteristics. Additionally, DWC reduces most of the non-technical problems that occur in EV, like the cost, size, and weight of the battery [7,36,105]. This charging concept confines the magnetic coupling between the primary coil below the floor's surface and the secondary coil installed under the vehicle chassis. Figure 8 shows the schematic diagram of DWC.

Here in the above schematic of DWC, the energy source is taken from solar energy and stored in the battery with the help of Maximum Power Point Tracking. The stored power can be transferred during the vehicle's arrival [146,150]. The primary coils are placed on a road signal or toll plaza track, which can continuously transfer power to the receiver coil fixed in the vehicle. After receiving the energy through the receiver coil and being suitably conditioned, the energy is stored in the EV battery. Low-powered DWC systems can be developed by using an embedded-based receiver coil. However, this technique is unsuitable for EV applications [36].

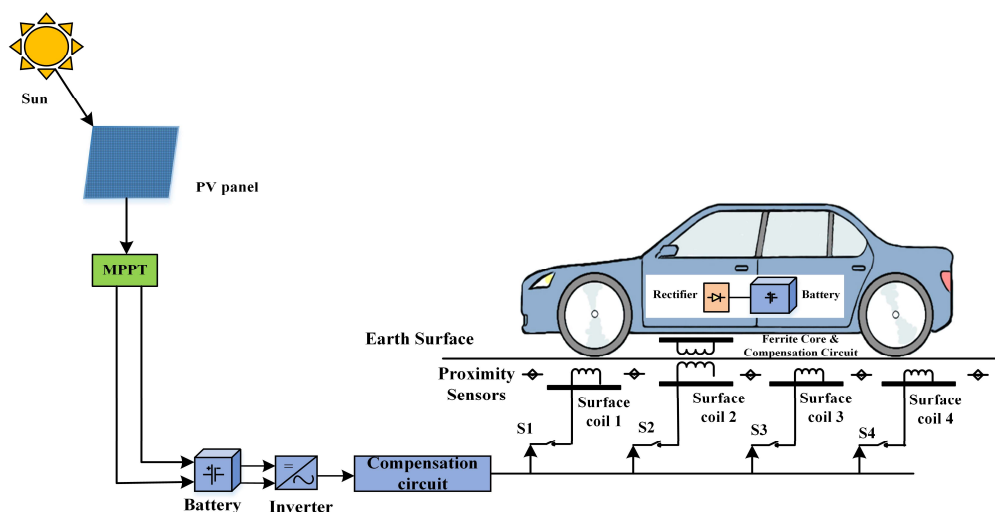


Figure 8. Schematic diagram of DWC.

Another aspect of the DWC is charging tracks, which come in two types based on their shape. The first type comprises a stretched track. A transmission coil’s dimension is considerably higher than the receiver coil’s. The second type of dynamic charging track is of a lumped shape. It is developed with a series of aligned coils having the same dimension as the pickup coil. This type of coil arrangement is also called a Grouped Periodic Series Spiral Coupler (GPSSC). A GPSSC-based dynamic coil arrangement can improve the coupling coefficient. Further, the efficiency of the dynamic charging is based on the coupling coefficients of the transmitter and receiver coils. Table 4 compares the WPTs available in modern EVs [151–153].

Table 4. Comparison among WPT in modern EVs.

Name	Frequency (Hz)	Efficiency (%)	Airgap (cm)	Year	Power (kW)	References
KAIST KAIST KAIST KAIST	20 k	71–85	1–20	2013	60	[154]
	20 k	80	15	2014	5–15	[155]
	20 k	71	20	2015	22	[156]
	20 k	74	20	2015	27	[7]
ORNL		90	25.4	2016	20	[157]
KRRI	60 k	82.7	5	2012	818	[158,159]
WAVE	23.4 k	92	17.8	2014	50	[155]
Qualcomm	20 k	-	-	2012	7	[160]
Fraunhofer	100 k	97	13.5	2014	22	[161]
Showa Aircraft Co.	22 k	92	15	2009	30	[142]
UM Dearborn	80 k	96	20	2014	7.7	[162]
	95 k	95.3	15	2015	6	[163]
	1 M	95	15	2015	3.3	[164]
WiTricity Human body Sim	13.6 M	NA	5–200	2007	0.06	[137]
NYU	85 k	91	21	2015	25	[165,166]

Table 4. Cont.

Name	Frequency (Hz)	Efficiency (%)	Airgap (cm)	Year	Power (kW)	References
Conductix Wampler	20 k	90	4	NA	120	[167]
WiTricity EV	NA	90	18	2015	3.3	[168]
INTIS	35 k	90	15	2011	30	[7]
Conductrix—Wampler	NA	90	4	2013	60	[169]
Utah State University	NA	>90	15	2012	25–50	[170]
Tokohu University	360 k	75	0–200	2012	0.015–0.018	[171]
Saitama University	50 k	94	7	2011	0.0015–0.003	[172]
University of Auckland	20 k	NA	20	2011	2	[173]
	20 k		10–25	2013	2–7	[122]
	85 k	91.3	10	2015	1	[174]
ETH Zurich	1 M	96.5	5.2	2015	5	[175]
	85 k	95.8	10–20	2015	50	[126]
Setsunan University	1.20–2.45 G	20–98	5–20	NA	NA	[176]
PATH	20 k	60	7.5	NA	60	[142]

NA—Not Applicable.

Shin et al. have initiated EV research on stretched tracks at the Korea Advanced Institute of Science and Technology (KAIST). The lumped track has been implemented at Auckland University [119]. In a lumped track, part of the lane does have the transmitter coil, which is coupled to the receiver coil. This type of arrangement is commonly called segmentation. It is beneficial to improve the efficiency of dynamic charging and neglect the radiation of electromagnetic fields. In dynamic charging, more concentration is needed in calculating the specified length of the coils in a stretched track to avoid the misalignment problem [151]. In lumped tracks, we need to concentrate more on the distance between each transmitter and receiver coil [177]. During dynamic WPT, the EV should travel at a constant speed and straight direction. Therefore, each track coil should be placed at a constant distance and supplied with a constant magnitude and sine wave current. Furthermore, the pickup and track coils should have the same coil structure and core material dimensions. These are all the conditions for dynamic WPT systems. The comparison of the various charging types is presented in Table 5. It shows that inductive power transfer is more suitable for domestic EV charging applications. Still, it has a minimal distance of power transferring capacity.

Quasi-dynamic WPT systems can easily be implemented on static and dynamic charging planes. Young Jae Jang et al. [152] discussed that quasi-dynamic charging-based vehicles could charge the battery in slow-moving, stationary, or moving conditions. They also compared and analyzed a cost-effective system among all charging systems and implemented an optimized static, dynamic, and quasi-dynamic wireless charging model. These quasi-dynamic charging systems are mainly helpful for public transportation vehicles like buses, autos, and cars. Traffic signals and bus stops are the perfect places for installing quasi-dynamic charging, where we can place the primary coils at a certain constant distance. Every coil has individual converters and controllers for turning on and off and is connected to traffic signals. The basic principle behind this charging is auto-detection and an advanced control strategy of charging fixed on the charging lane, whether static or dynamic. For example, if the quasi-dynamic charging-based vehicle moves on the dynamic

charging lanes, it should charge its battery dynamically. Likewise, if the dynamic charging lane is unavailable, the same vehicle should change the charging mode to static. Therefore, these charging systems require higher control systems to detect the charging method automatically. A. Mohamed et al. have implemented and validated a model of quasi-dynamic wireless charging [95]. This implementation includes three types of analysis: (i) we can charge the EVs at a constant power level, which improves driving range and increases efficiency; (ii) different charging levels of power; and (iii) V2G and G2V techniques were also tested. This charging system is very suitable for electric buses because buses will stop at a fixed distance for stops. KAIST explained quasi-wireless charging systems for buses on their website with some videos.

**Table 5.** Comparison of the different charging types of EVs.

Charging Type	Distance	Technology	Power	Efficiency	Comments
Electro magnetic field	Near-Field	Inductive Power Transfer [7,125–143]	High	High	Distance of power transfer is minimal and efficient.
		Coupled magnetic resonance [116–121]	High	High	Suitable for EV application.
Electric Field		Capacitive Power Transfer [109–115]	Low	High	Power and distance are too short for EV applications
Mechanical Force		Magnetic gear [129]	High	High	Suitable for EV charging
Wave Energy	Far-Field	Radio wave and microwave [5,96–100]	High	Low	Efficiency is very low for power transfer applications
		Laser [101–104]	High	Low	It required a straight line for the path of transmission and an important tracking mechanism.

#### 4. Coil Structures

Maintaining proper alignment between the primary and secondary coils is mandatory for an efficient inductive power transfer system. The misalignment can occur in the charging pads' horizontal, vertical, and angular shapes. The coil misalignment problems are occurring in various situations and various types of applications. As a result, mutual inductance, efficiency, and output power will change during the operation. The maximum misalignment problems will occur with improper parking of the EV and mismatching between the primary and secondary coils. This misalignment of coils increases magnetic flux leakage, mismatches of impedance values, and mutual inductance defragmentation. However, maximum power transfer efficiency can be achieved by improving the quality factor and coupling coefficient. The different research articles proved that three solutions are available to improve the power transfer efficiency, quality factor, and coupling coefficient [178,179].

Firstly, there ought to be proper alignment of the transmitter and receiver coils. This state requires exact positioning from the driver or mechanical alignment system with the primary and secondary windings. This is the main drawback of the IPT system. Different methods were proposed in the literature to tolerate the misalignment problems and maintain the efficiency of various coupling factors. The unique approach called Parity-Time Symmetric (PTS) circuit-based WPT system has recently been implemented to maintain the constant output power and transfer efficiency without relating to the coupling coefficient [180]. The PTS method works based on the quantum physics concept at the PTS region. It consists of coupled parallel LC circuits [181,182]. Generally, PTS systems are applicable for low-power applications (less than 1 kW). While the PTS system is used in high-power applications, we must overcome higher current and voltage stress, coil ohmic losses, and switching losses. Therefore, this method can be appropriate only for static charging and not for dynamic charging of EVs [183,184].

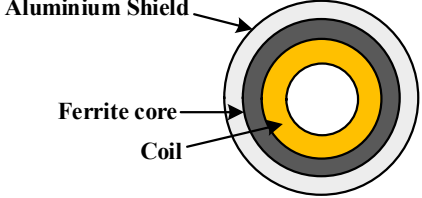
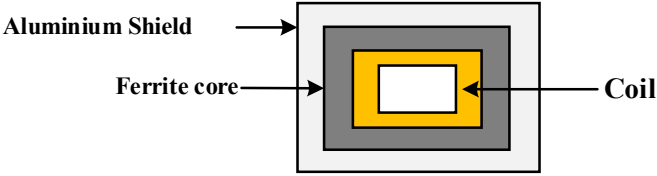
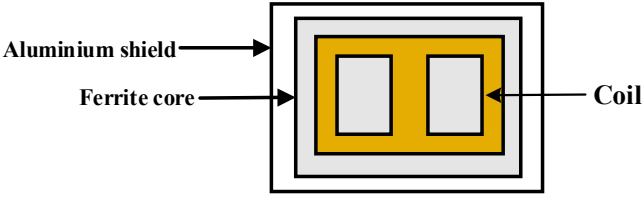
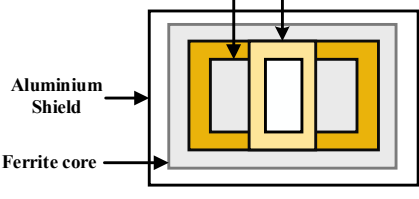
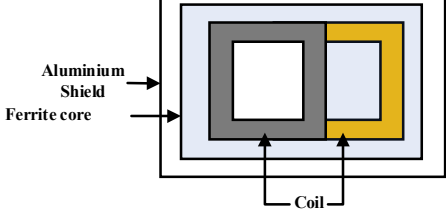
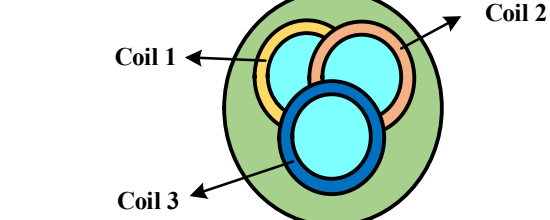


Secondly, use of different shapes of charging pads and coil designs to minimize misalignment problems, like cone-shaped, coaxial-shaped, arc-shaped, and ring-shaped coils [185], recently, some anti-misalignment techniques were proposed by EV researchers. The anti-misalignment techniques can be achieved using phase angle optimization, the balanced particle swarm optimization method [186], and electromagnetic induction position sensors. The phase angle optimization method tolerates misalignments from  $-200$  mm to  $+200$  mm. The different pad positions' phase angles can be compared with the predefined phase angle value and then adjusted with the proper value [187]. The electromagnetic induction position sensors are fixed in the receiver pad, and the screw or servo motor setup is attached to the transmitter pad. Based on the position sensors output, the motors can align the transmitter and receiver pads [188]. Lastly, proper electrical manipulation techniques, such as compensation topologies, are used because of the high airgap between the primary and secondary coils.

These three solutions are briefly explained in the following sections. Using the Finite Element Analysis (FEA) method eases the implementation of the amount of magnetic field extracted for a particular coil design and temperature extraction from the coil [189]. Separate research will improve the efficiency and minimization of charging pad size by using different core shapes and the proper shape of the coil design. E-cores [190], U-cores [190,191], and pot cores [192,193] are the three basic designs of magnetic cores for charging pads. Primary and secondary coils should be placed on the ferrite core material. This ferrite core material is also one of the important safety parameters for wireless charging. The magnetic flux leakages can be reduced by using appropriate shapes of resonators and ferrite core materials [194]. The coils' size and shape, the medium's permeability, operating frequency, and cost are the basic factors for selecting ferrite core materials for core design. However, these ferrite cores will affect the coupling between the primary and secondary coils. Circle, square, and rectangle are the fundamental shapes of the ferrite core material [195–197]. Different shapes of coils have their merits for their respective applications. However, they may increase the weight of the charger and cause lateral misalignments. These shapes of the cores are not suitable for EV applications. Various cores or resonator shapes have been implemented to overcome these drawbacks of basic core shapes.

The structure follows two types of planar coils: Polarized Pads (PPs) and Non-Polarized Pads (NPPs). PPs are DDQ, DDQP, and Bi-Polar (BP). It can create both parallel and perpendicular magnetic flux [133]. NPPs are single-layer pads, like circular and rectangular ones. They may allow the magnetic flux to flow in a vertical direction. Various coil designs, structures, and shapes have been discussed, along with their efficiencies and simulations. A 2 kW WPT system was implemented with a 700 mm airgap between the coils. Adding additional current-carrying primary windings can easily improve the coupling between the primary and secondary coils. Plastic materials can be used in WPT for external protection in coil structures. Aluminum shielding supports coil pads and protects the environment from the EMF extracted from coils. Daniel Ongayo et al. compared the flux linkage between the circular and rectangular coils and confirmed that circular coils have higher transferring efficiency. However, circular coils have some drawbacks when increasing the airgap between the coils, i.e., we can easily achieve higher efficiency with a lower airgap. However, if we expand the airgap by one, we need to increase the diameter four times [133]. DD, DDQ, DDQP, and BP are introduced to overcome the drawbacks of circular coils [9,10,79,133]. The different coil structures for wireless charging are shown in Table 6. All types of coil structures can be used for static and dynamic charging. The system's efficiency will depend on the direction and intensity of the generating magnetic flux and its alignment. Circular coils are not fit for dynamic charging due to the 38% horizontal offset of the coils. Every coil structure has been briefly explained in the upcoming sections.

**Table 6.** Coil structures for wireless charging.

S. No	Coil Structures
1	<p style="text-align: center;"><b>Polarized pad circular</b></p> 
2	<p style="text-align: center;"><b>Polarized Rectangular pad</b></p> 
3	<p style="text-align: center;"><b>Non – polarized pad Double D - coil</b></p> 
4	<p style="text-align: center;"><b>Non – polarized pad Double D quadrature coil</b></p> 
5	<p style="text-align: center;"><b>Non – polarized Bi polar Double D – coil</b></p> 
6	<p style="text-align: center;"><b>Tripolar pad</b></p> 

#### 4.1. Polarized Pad Circular Coil

The circular design of the coil is widely used in static charging [6]. Compared to other models, it has lower coupling during identical airgaps and misalignments. The tolerance of the coupling capacitor is the same during misalignment in all directions [87,163]. Due to the flux cancellation, the magnetic null characteristic affects the system. Dynamic WPT can also use this phenomenon with proper arrangements.

#### 4.2. Polarized Rectangular Pad

This type of coil arrangement can reduce flux leakage and increase the flux area [178]. This coil design can be most preferred for dynamic wireless charging applications [6,62,136]. It has better tolerance, a lower weight, and a compact and simple design [183,184].

#### 4.3. Non-Polarized Pad Double-D Coil

This type of arrangement creates a single-sided flux path with less flux leakage and a parallel component to the flux [83]. The added advantages of this coil are its smaller size, lightness, and greater tolerance of misalignment in the horizontal direction [110,169,184,189].

#### 4.4. Non-Polarized Pad Double-D Quadrature Coil

The flux's vertical and horizontal components can be generated in DDQP coils. Addition of a quadrature coil to the DDP to form the DDQ. A pair of synchronized inverters and rectifiers for primary and secondary pads are needed, respectively [198].

#### 4.5. Non-Polarized Bi-Polar Double-D Coil

D-shaped coils effectively work during misalignment issues. DDQP and BP pads alternatively work with other types of pads and have a higher tolerance for misalignment [190,191].

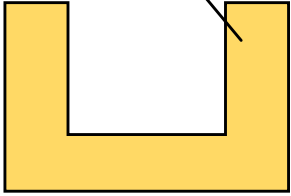
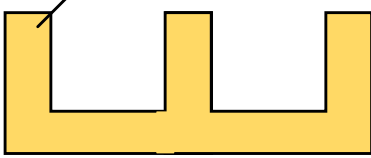
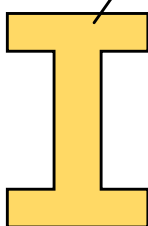
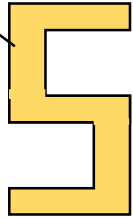
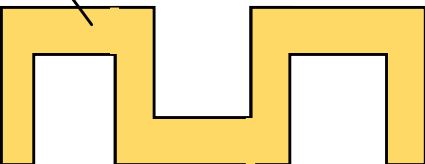
#### 4.6. Tripolar Coil

Three different coil arrangements are mutually decoupled from each other [192,193]. The coupling factor and coefficient of coupling are higher when compared to other bipolar pads [196,197,199–201]. It is flexible in high rotational misalignment and has a less leaky magnetic field [202,203].

#### 4.7. Single-Layer Coils

The system is made easier and less expensive by the long-track transmitters [156,204–208], which are significantly longer than the EV length and only need a single power inverter and one adjustment tank. The ferrite core shape for the long-track transmitter serves as the inspiration for the name of the single-winding topology. The single-winding topologies are shown in Table 7. Because the reception coil only partially encloses the lengthy transmitter coil, the poor coupling coefficient is acknowledged as the system's primary flaw. This causes a poorer efficiency profile and more stray magnetic fields. Numerous studies are carried out to address the stray field issues and also to streamline the magnetic shielding design [156,205–210]. For instance, I-type and S-type transmitters with widths of 10 cm and 4 cm, respectively, are suggested in [156,207] to further narrow the transmitter coil width. Additionally, by switching the magnetic polarities of nearby poles, stray fields can be significantly minimized [207]. In a subsequent development, an N-type transmitter is suggested in [209] to further reduce the volume of the ferrite core while keeping the benefits of the I-type structure. However, further research reveals that, depending on the receiver's position in the driving direction, the magnetic flux density produced by I-type, S-type, or N-type transmitters on a single receiver fluctuates in a roughly sinusoidal function. According to [206], the magnetic flux density increases to its highest value at the center of each ferrite pole and decreases to almost zero in the center between two adjacent poles. As a result, the induced voltage and received power vary dramatically depending on where the EV is located. In some places along the EV's path along the transmitter, the received output power drops to almost zero.

**Table 7.** Single-layered coil structures for wireless charging.

S. No	Coil Shapes
1	<p data-bbox="930 353 1043 383">U - Shape</p> <p data-bbox="1082 353 1291 383">Ferrite core with coil</p> 
2	<p data-bbox="930 645 1139 674">Ferrite core with coil</p> <p data-bbox="1209 645 1331 674">W - Shape</p> 
3	<p data-bbox="970 898 1075 927">I - Shape</p> <p data-bbox="1139 898 1307 927">Ferrite core with coil</p> 
4	<p data-bbox="970 1205 1075 1234">Ferrite core with coil</p> <p data-bbox="1209 1205 1310 1234">S - Shape</p> 
5	<p data-bbox="890 1473 1011 1503">Ferrite core with coil</p> <p data-bbox="1209 1473 1326 1503">N - Shape</p> 

#### 4.7.1. U-Shape Coil

The U-shape coils are used with Double-D coils for performance analysis, and U-shape and Double-D coils are used as a transmitter and receiver, respectively. In these coils, there is no change in the magnetic polarity of nearby poles. The efficiency can be achieved at 72% with an airgap of 17 cm. However, higher rail field emission may arise due to weakly conducting characteristics [206,207].

#### 4.7.2. W-Shape Coil

W-shape coils are tested with multiphase W-shape coils. During power transfer, there is no change in the magnetic polarity. Additionally, these coils attain an efficiency of up to 80% in a 26 cm airgap. However, it is affected by the higher stray field emission due to the soft conductivity and uncapped shapes. It requires reactive power shielding to avoid losses and achieve maximum efficiency [205].

#### 4.7.3. I-Shape Coil

I-shape coils performance has been checked with Double-D coils on the receiver side. There is a change in the magnetic polarity at the coils while transferring the higher range of power. This coil shape can be efficient in misalignment (up to 24 cm), but with stray field emission dynamic charging, it will be affected by higher fluctuations. It can attain an efficiency of 74% in an airgap of 20 cm [156,205–209].

#### 4.7.4. S-Shape Coil

Similarly, S-shape coil performance was also verified with the help of Double-D coils. There is a change in the magnetic polarity at the alternative poles of the coils. S-shape coils can maintain their efficiency at higher misalignments (up to 30 cm) and with stray field emission. I-shape coils can give 71% efficiency in a 20 cm airgap. It is slightly smaller than other coils [156].

#### 4.7.5. N-Shape Coils

N-shape coils have experimented with multi-winding coils. During power transfer, there is a change in magnetic polarity at the alternative poles of the coils. It reduces the ferrite core size compared to an I-shape coil. Due to the reduction of the ferrite core, stray field emission is eliminated. This shape of coil is also affected by the high-power fluctuation in dynamic charging [209].

The different coil designs can be simulated using the ANSYS and COMSOL software, and then the appropriate magnetic field exposure can be easily calculated. The coupling coefficient values can be used to compare the simulation results of various coil structures in different misalignment problems. Commonly, bipolar pads have a higher coupling coefficient and misalignment tolerance. The coupling coefficients are inversely proportional to the number of aluminum shields. The comparison of various coil arrangements with different magnetic characteristics is depicted in Table 8. From this comparison study, among all the coil shapes, bipolar and circular coils are the most suitable selections for EV applications [163,171]. Circular coils give good performance with aluminum shielding in a single-sided flux pattern and are easy to implement. Bipolar coils tolerate the higher misalignment problems with double-sided shielding than circular coil design and exposure to minor magnetic fields [123].

**Table 8.** Comparison of various coil arrangements with different magnetic characteristics.

Structure of the Coils	Misalignment Tolerance	Coupling Coefficient	Magnetic Field Leakage	Shielding Effect on the Coupling Coefficient	Magnetic Flux
Circular pad [175]	Much less	Less	More	Less	Single side
DD Coil [167]	Much less	More	Less	More	Double side
DD-Q Coil [127]	More	More	Less	More	Double side
BP pad [91]	Average	More	Less	More	Double side
Tripolar pad [198,211–214]	More	More	Less	Less	Single side

## 5. Operating Frequency

The operating frequency and power level are the two significant parameters for improving the efficiency and airgap of the wireless charging of EVs. Therefore, modification of the operating frequency may change the system into a simple and efficient one. On the other hand, if the WPT frequency increases, the efficiency will also increase, but there will be a limitation in power level. Therefore, these two factors are related to each other. Other than these two factors, there is no standard development for optimizing the WPT efficiency.

Different universities, research centers, and automobile industries are currently concentrating on the wireless charging concept and targeting better EV solutions. They aim to design a standardized system that is efficient for all users. Typically, WPT systems use an operating frequency of about 1 MHz for high-power applications [198]. The experimental system was developed with a frequency range of 100 kHz–200 kHz. Zhang et al. [164] have explained the transfer quality factor  $T_o = \omega M/R_o$  where  $R_o$  is the equivalent resistance,  $\omega$ , and  $M$  are the resonant frequency and mutual inductance, respectively. The following requirements must be satisfied to achieve optimal transfer quality: (i) The power electronics circuit's switching frequency values must be adaptively stable to maintain the highest transfer power. The switching frequency and the resonant coil design significantly contribute to the high efficiency of the WPT system, (ii) The switching frequency and duty ratio can be calculated using the coupling coefficient between the primary and secondary coils. The coil size must be reduced as the switching frequency increases to maintain a high coupling factor. So, achieving high levels of mutual inductance and coupling coefficient is essential. This will be accomplished by correctly aligning the two coils [212], and (iii) the equivalent resistance should be low. Furthermore, the resonant frequency can be derived from  $\omega = 1/\sqrt{LC}$  where  $C$  is capacitance and  $L$  is inductance [213]. The suitable compensation topologies can attain the optimal transfer quality factor conditions. Consequently, the optimal switching frequency for WPT depends on various factors, such as the size of the coils, the airgap between the coils, and the power transfer rate. The optimal switching frequency for a specific WPT application is determined by considering the coupling factor, switching losses, and other system parameters [214].

## 6. Compensation Topologies

Inductively coupled systems provide a considerably lower efficiency compared to resonance-based IPT systems. The large distance between the transmitter and receiver coils produces a higher leakage inductance value. It reflects in the efficiency, which decreases by below 50%. This leakage inductance can be overcome by adding additional compensating capacitors in the transmitter and receiver [215]. Based on a proper compensation network, better efficiency can indeed be achieved in cases of high misalignment problems. The specified reasons for compensation topologies are:

- To generate reactive power at primary and secondary coils, which is required to generate a proper magnetic field. Additionally, primary coil compensation topologies are used to reduce the voltage and current ratings of input supply power, and secondary coil compensation topologies are used to improve the ability to transfer the power [216];
- To maintain the constant current and voltage [217];
- The coupling coefficient and quality factor can decide the maximum efficacy of the WPT system [218].

Compensation topologies are divided into two categories based on the capacitor's place in the circuit. They are subdivided into different types.

### 6.1. Basic Compensation Topology

Basic compensation topologies are divided into five types and shown in Figure 9. They are named as Series-Series (SS) [179,219–223], Series-Parallel (SP) [224], Parallel-Parallel (PP) [225], Parallel-Series (PS) [226], and Series-Parallel-Series (SPS) [227].

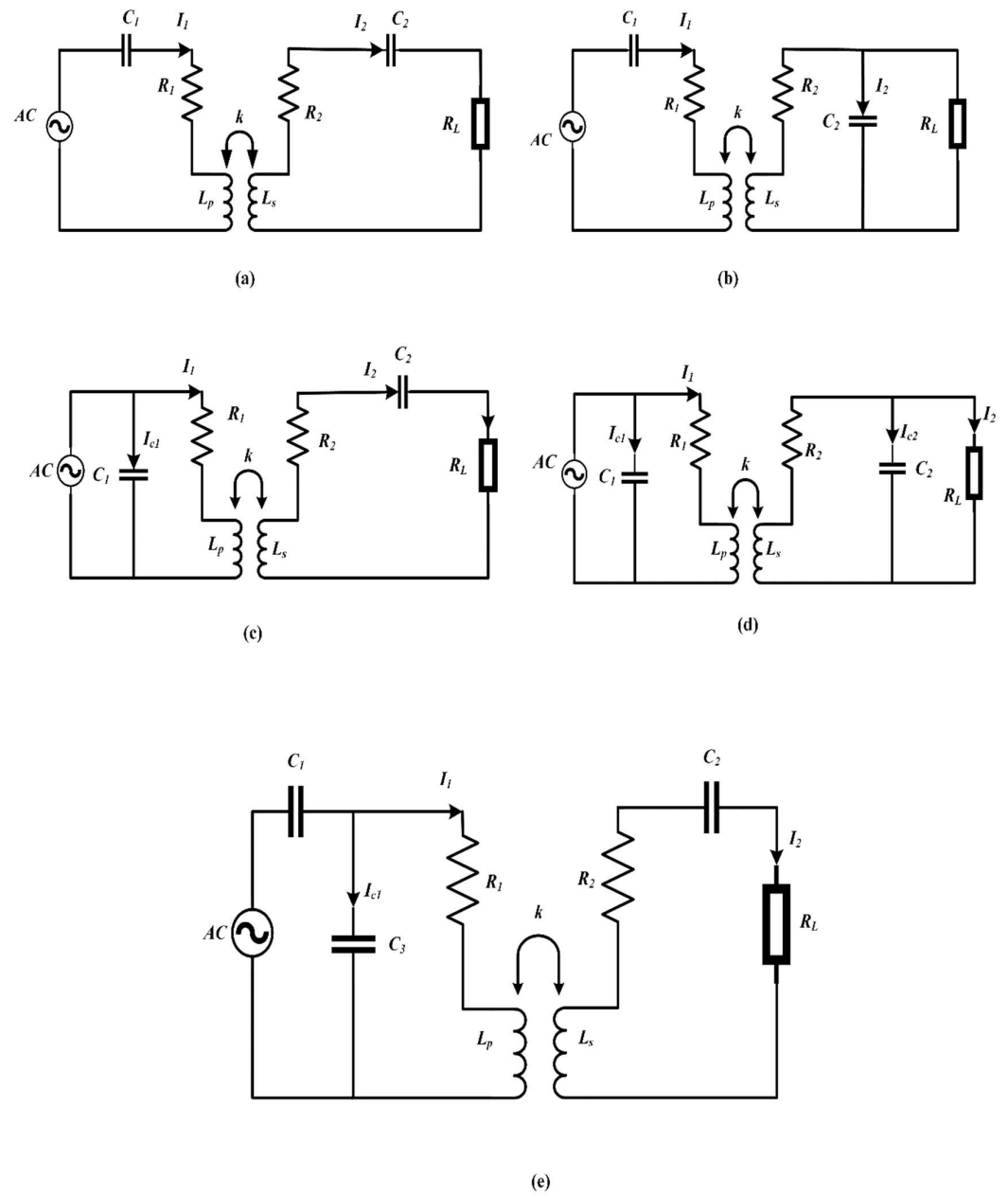


**Figure 9.** Basic compensation topologies: (a) Series-Series (SS); (b) Series-Parallel (SP); (c) Parallel-Series (PS); (d) Parallel-Parallel (PP); and (e) Series-Parallel-Series (SPS).

In Figure 9,  $k$  denotes the coupling coefficient, and  $L_p$  and  $L_s$  are the self-inductance of the transmitter and receiver coils, respectively.  $C_1$  and  $C_3$  are transmitter coil compensation capacitors.  $C_2$  is the receiver coil compensation capacitor. Primary and secondary side resistances are  $R_1$  and  $R_2$ , respectively.  $I_1$  and  $I_{c1}$  are transmitter-side input currents.  $I_2$  and  $I_{c2}$  are receiver-side output currents.  $R_L$  is the resistive load. The selection of these compensation circuits can vary concerning the application levels [181,228].

### 6.1.1.1. Series-Series Topology

For constant current output and constant voltage applications, an SS combination can be used [181]. The operating frequency level is the same for constant-current operations. Economically apt for high-power applications [227–231]. Suitable for variable load condi-

tions and high-power applications,  $\omega = 1/\sqrt{L_1 C_1}$ . Less copper is enough for operation. The final equation of *SS* topology is shown in (2).

$$\overline{Z}_{Total} (SS) = \left( R_1 + j \left( L_p \omega - \frac{1}{C_1 \omega} \right) \right) + \frac{\omega^2 M^2}{\left( R_2 + R_L + j \left( L_s \omega - \frac{1}{C_2 \omega} \right) \right)} \quad (2)$$

### 6.1.2. Series-Parallel Topology

*SP* is also most economically useful for high-power transfer applications. In addition, it is suitable for variable load conditions. It can work on both current and voltage sources. Therefore, it is well suited for high-power applications [232]. The final equation of *SP* topology is shown in (3).

$$\overline{Z}_{Total} (SP) = \left( R_1 + j \left( L_p \omega - \frac{1}{C_1 \omega} \right) \right) + \frac{\omega^2 M^2}{\left( R_2 + j L_s \omega + \frac{R_L}{1 + j R_L C_2 \omega} \right)} \quad (3)$$

### 6.1.3. Parallel-Series Topology

In *PS* topology, capacitors are connected in parallel and series with the transmitter and receiver coils. Therefore, the circuit's total impedance will increase during the misalignment problem, and a sudden decrease will occur at both the transferred and received currents [232]. The final expression of *PS* topology is shown in (4).

$$\overline{Z}_{Total} (PS) = \frac{1}{\left( R_1 + j L_p \omega \right) + \frac{\omega^2 M^2}{\left( R_2 + j \left( L_s \omega - \frac{1}{C_2 \omega} \right) \right)}} + j C_1 \omega \quad (4)$$

### 6.1.4. Parallel-Parallel Topology

This topology contains a set of capacitors connected separately in parallel with transmitter and receiver coils [232]. As a result, both the transmitter and receiver coils have a large impedance value. The final equation of *PP* topology is shown in (5).

$$\overline{Z}_{Total} (PP) = \frac{1}{\frac{1}{R_1 + j L_p \omega} + \frac{\omega^2 M^2 (1 + j R_L C_2 \omega)}{(R_L + (R_2 + j (L_s \omega - \frac{1}{C_2 \omega})) (1 + j R_L C_2 \omega))}} + j C_1 \omega \quad (5)$$

### 6.1.5. Series-Parallel-Series Topology

*SPS* is a combined topology of *SS* and *PS*. System change into *PS* topology at  $K = 1$ . The condition for rating misalignment is to maintain  $K_c$  [233]. The higher values of rated misalignment power can be obtained at lower  $K_c$  values. The equation for *SPS* topology is shown in (6).

$$\overline{Z}_{Total} (SPS) = \frac{\overline{Z}_{11}}{1 + Z_{11} j C_3 \omega_0}, \text{ where } \overline{Z}_{11} = \overline{Z}_1 + \overline{Z}_P \quad (6)$$

## 6.2. Hybrid Compensation Topologies

Popular hybrid compensation topology combinations are shown in Figure 10, such as LCL-P [234], LCC-P [235], S-CLC [236], CCL-S [237], LCL-S [238], LCC, LCC-LCC [169,239–241], double-sided LCC [235], and LCL-LCL [236]. These combinations are denoted as primary and secondary sides.



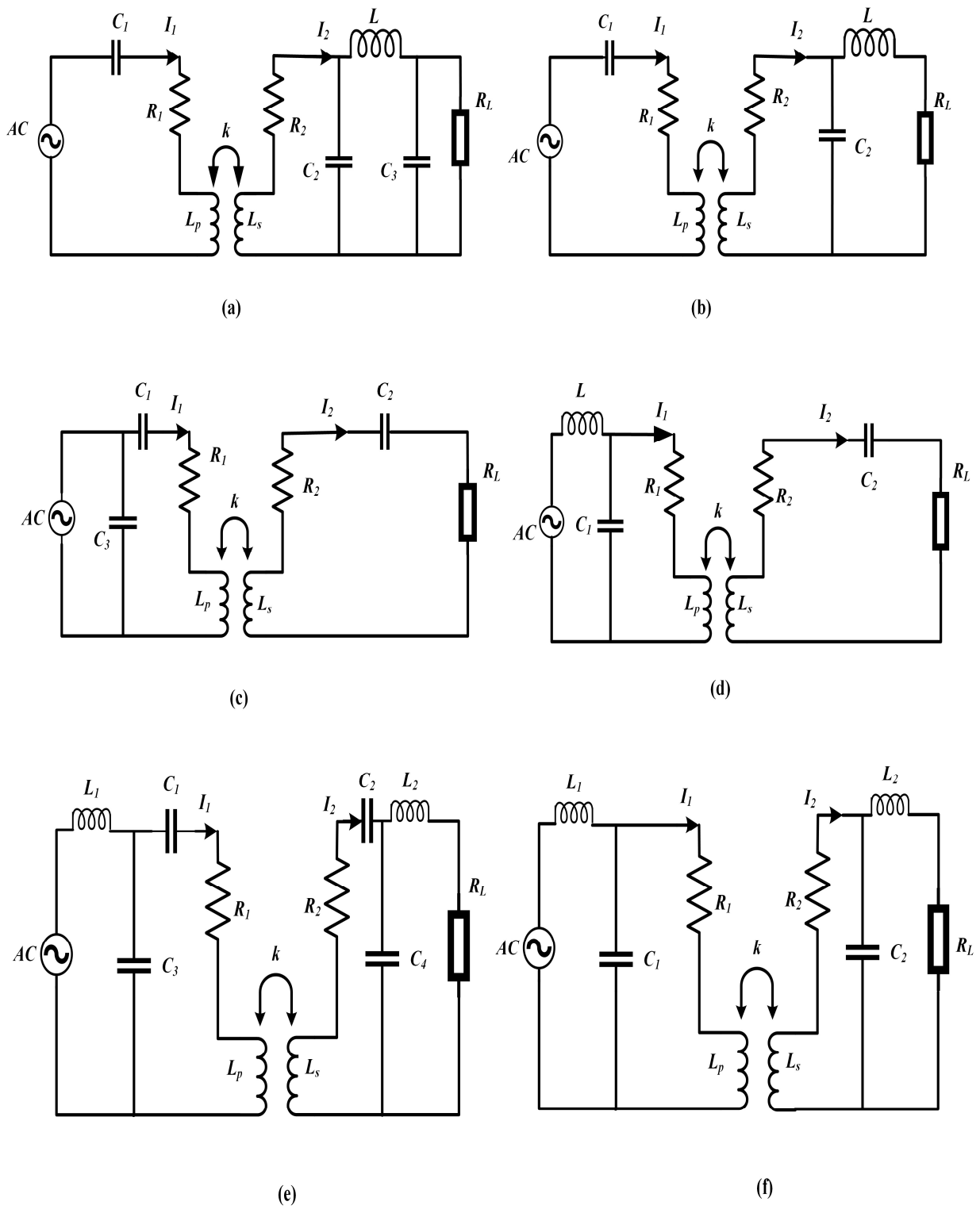
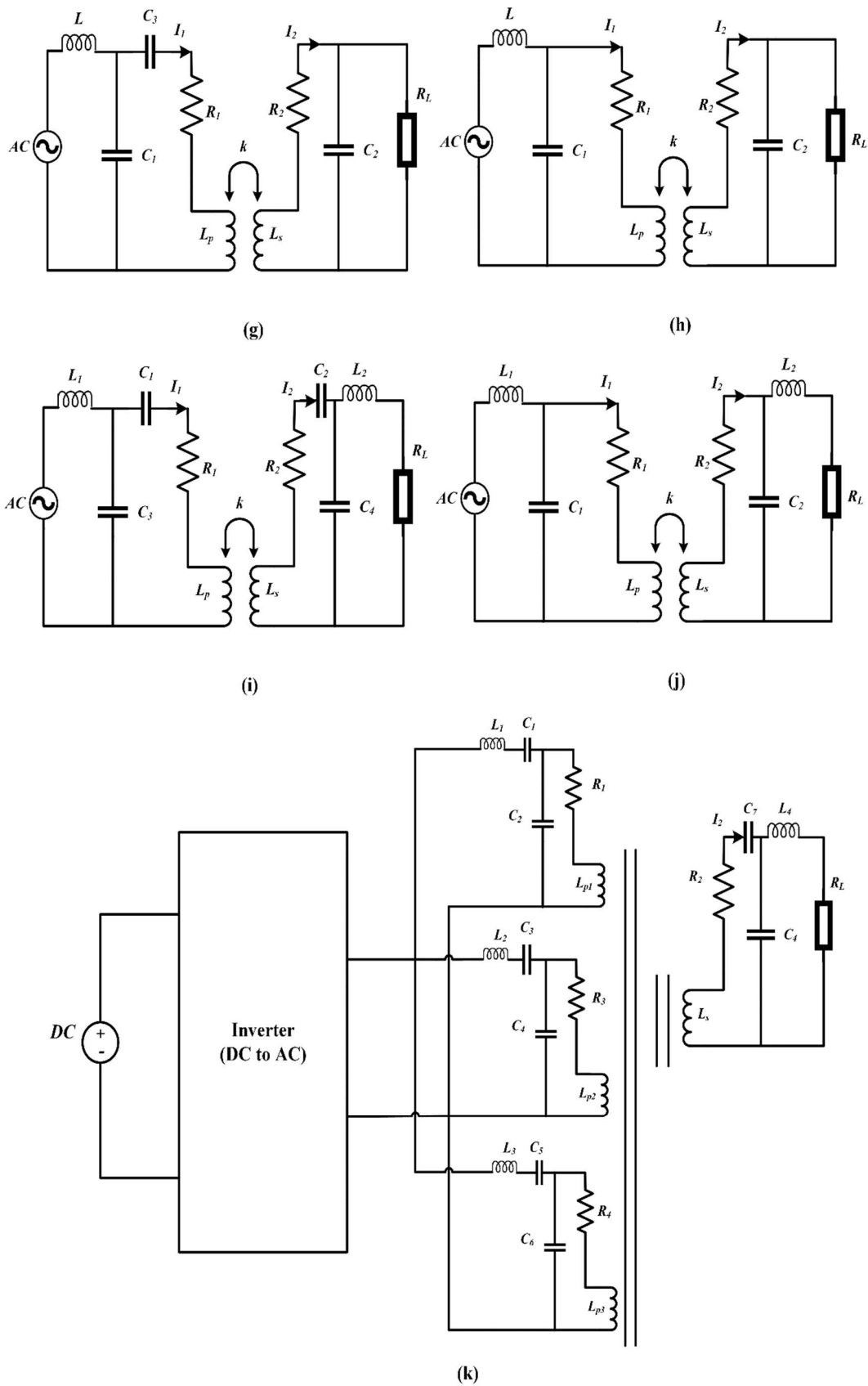


Figure 10. Cont.



**Figure 10.** Hybrid compensation topologies: (a) S-CLC; (b) S-LCL; (c) CCL-S; (d) LCL-S; (e) LCC-LCC; (f) LCL-LCL; (g) LCC-P; (h) LCL-P; (i) LCC-S; (j) LCC; and (k) double-sided LCC.

The PS compensated topology, one of the basic compensation topologies, has a reduced current rating and reduced conduction losses of the switching devices for any value of power level. Additionally, the voltage stress on the inverter switches is very high, particularly at higher power loads. It can worsen the condition at lower values of the coupling coefficient. CCL-S is one of the hybrid topologies and is shown in Figure 10c. This topology can easily eliminate the switching losses likened to the parallel LC-S topology with the help of an additional primary series capacitor. Parallel LC compensation topologies can be applied for lower-level voltage gain applications. CCL-S is preferred for higher voltage gain applications. S-CLC topology can easily achieve the zero-phase angle, as shown in Figure 10a. Figure 10k shows the double-sided LCC topology, which is mainly suitable for continuous power delivery applications like dynamic WPT. Table 9 shows the various compensation topologies with different WPT applications [242]. There are seven combinations of compensation topologies that have been compared with one another based on the power ratings, operating frequency, and airgap. According to the comparison, LCC-LCC and LCC-SS are efficient topologies for the static WPT technique. However, using these topologies, managing the power loss problems in high power transfer is mandatory.

The SP, S-LCL, S-CLC, and SS output voltage and current are in a topsy-turvy relationship with the mutual inductance. The output power is determined by the topsy-turvy relationship with the square value of the mutual inductance. However, the output current and voltage of the PP, PS, double-sided LCC, double-sided LCL, LCL-S, and LCL-P maintain a direct relationship with the mutual inductance. The output power is directly related to the square value of the mutual inductance. Accordingly, the design methods can be determined for compensation topologies. SS-compensated WPT systems are developed to share nominal power at the high value of mutual inductance; primary and secondary resonators are perfectly aligned. Additionally, LCC-compensated systems are developed to share nominal power at a lower value of mutual inductance, that is, a higher misalignment between the primary and secondary coils. Table 10 compares the different compensation topologies with various dynamic WPT applications [242]. The LCC-S and double-sided LCC topologies can efficiently handle higher misalignment problems in a dynamic WPT environment. It can achieve a power transfer efficiency of 93–98%. Still, the airgap is slightly short in these compensation topologies.

**Table 9.** Various WPT systems with different compensation topologies.

Compensation Topologies	$R_L$ ( $\Omega$ ), f (kHz)	Coupling Coefficient (k)	Output Power, Voltage	Efficiency	N1, N2	$D_1$ Length (mm)	$D_2$ Width (mm)	Airgap (mm)	Comments
SS/LCC-LCC [239,240]	$R_L = 2, 3, 5$ f = 85	0.135	1 kW, 50 V	95% in SS, and 93% in LCC	10, 8	500	400	200	LCC-LCC compensation is more reliable for the electromagnetic field interface.
SS/LCC-LCC [241]	f = 85	-	7.7 kW 270–405 V	96% in LCC		800	600	200	At lower values of mutual inductance, the LCC compensation has more efficiency.
SS/LCL-LCL [243]	$R_L = 10$ f = 85	0.1	3.3 kW	93.1% in SS, 90% in LCC	$20 \times 3, 17 \times 2$ layers	$550 \times 400 \text{ mm}^2$	$240 \times 240 \text{ mm}^2$	100	LCL-LCL compensation has a higher power factor value compared to SS.
LCC-LCC [244]	f = 79 $R^L = 10\text{--}200$	0.18–0.32	7.5 kW 450 V	96%	1	800	600	200	Resonant frequency (f) is not dependent on the load conditions or coupling coefficient.
LCC-LCC [245]	f = 95	0.14–0.30	5.6 kW 300–450 V	95.36%	-	600	600	150	More induced couplings to increase the space between magnetic cores.
LCC-LCC [246]	f = 85 $R^L = 49.95$	0.153	3.3 kW 405.7 V	92.6%	18, 16	600	300	150	The battery has only a relationship with transmitter power and coupling coefficient, not with the compensation circuit.
LCC-LCC [247]	f = 85	0.1877	3 kW 300 V	95.5%	-	$600 \times 450 \times 4 \text{ mm}^3$ $640 \times 496 \times 8 \text{ mm}^3$	$400 \times 300 \times 4 \text{ mm}^3$ $480 \times 352 \times 8 \text{ mm}^3$	150	A smaller level of transmitter and receiver design helps to neglect the extra-coupling effects.

**Table 10.** Various dynamic wireless charging systems with different compensation topologies.

Compensation Topologies	Resonant Frequency (kHz)	Coupling Coefficient (k)	Output Power, Voltage	Efficiency	Number of Turns and Dimensions of the Coils	Airgap (mm)	Comments
LCL-S LCC-S [248]	140	0.18–0.32	1 kW, 90 V	LCC and LCL: 93%	Radius of the coil: 163 mm.	100	This compensation gives drastic transfer characteristics at different quality factor values.
Double-sided LCC [249]	85	0.13	7.7 kW 270–405 V	96% in LCC	Transmitter: 9 turns, 6 × (388 × 400 mm). Receiver: 9 turns, 485 × 400 mm.	150	This compensation topology is more suitable for reducing the power fluctuations of dynamic wireless charging.
LCL [250]	85	0.037–0.054	5 kW	-	Transmitter and receiver: 350 mm × 700 mm.	240	By switching on the single primary coil, you can transfer the power throughout the track.
SS [251]	79	0.4	20 kW	80%	Transmitter: 9 turns, 10 cm × 75 cm. Receiver: 12 turns, 25 cm × 20 cm.	100	This system uses a new downscale prototype instead of a real-time model, operating at a frequency of 85 kHz.
SP [252]	23	-	2 kW	95.36%	Transmitter: 7 turns, 330 mm diameter. Receiver: 5 turns, 330 mm diameter.	100	There are different types of dynamic charging, like power variations due to positions and the decrement of the magnetic field below the safe limits with shielding effects.
SS [253,254]	85	-	-	97.6%	Transmitter: 8 turns, width is 58 mm. Receiver: 8 turns, width is 38 mm.	200	Using the Surface Impedance Boundary Condition technique to study the induced losses and investigate the different lengths.

## 7. Affecting Factors and Safety Considerations for WPT

Most EV consumers raise questions about the WPT systems, for instance, “whether these systems are safe or not” due to their higher range of electromagnetic field generation. Eric Giler said that WPT systems are much safer than mobile phone radiation [255]. H. Moon et al. proposed the new phase shifter by using a double shielding coil against magnetic flux leakage [256]. This type of double shielding creates an opposite field that eliminates flux leakage. WPT has many advantages in EV charging, like more convenience, cost, size, time, and power density. One of the remarkable advantages of wireless charging is that there is no need to make the charger port connection with the vehicle and disconnection after the vehicle leaves the charging lane location. The probable dynamic charging lanes in toll plazas and traffic signals could avoid the need to set up separate fast-charging infrastructure and batteries with a higher range. However, WPT needs to transfer more electrical energy (in kilowatts), adding more stress to the electromagnetic field. The higher value of EMF reduces the efficiency and reliability of the WPT system [257].

To overcome the EMF exposures, arranging the safety aspects on the transmission and receiving ends is mandatory [258]. It can be restricted with the help of a pacemaker-type arrangement over primary and secondary coils made using titanium or aluminum materials. This type of pacemaker is widely used in wireless charging-based medical equipment at low-frequency levels (20 kHz) [259–262]. Wireless charging experiences more limitations, predominantly on power transfer efficiency and the time taken to charge the battery, than plug-in charging. Massive power must be transferred within a 10–20 mm airgap. Several factors may affect the WPT. Its efficiency is typically concerned with the rudiments of airgap distance, system load, compensation topologies, coil dimensions, weight, alignment position of the coil, and frequency levels. Especially in dynamic wireless charging, vehicle speed, and proper control strategies, more close attention is required [219].

Apart from these technical hindrances, more attention must be paid before implementing this technology to the inevitable safety issues for humans during high power transmission through the air. Some problems, like an electric shock and fire accident, may occur due to the high-power cables and nearby electromagnetic fields. All EV manufacturers should follow similar prototypes for their vehicles and primary coil installations to overcome these safety problems. Those standard prototypes were developed by the International Electrotechnical Commission (IEC), the Institute of Electrical and Electronic Engineers (IEEE), SAE, the International Committee on Electromagnetic Safety (ICES), the International Commission on Non-Ionizing Radiation Protection (ICNIRP), and Underwriter Laboratories (UL) [229]. IEEE and ICNIRP fix the setpoints for magnetic field strength, operating frequency, and magnetic flux leakage for wireless charging [188]. The standardized prototypes for EV charging are shown in Table 11. The automobile manufacturers and research organizations are implementing the WPT technology, followed by standardized prototypes, and improving performance in a safe environment.

**Table 11.** Standard prototypes for EV charging.

Standard Developer	Standard Name	Published Date	Description	Status
IEC	IEC 61980-1 Ed. 1. 0-NEW ADDITION [258]	24 July 2015	EV Wireless Power Transfer Systems—PART 1: General Requirements	Withdrawn
IEC	IEC 61980-1 Ed. 2.0 [259]	19 November 2020	EV Wireless Power Transfer Systems—PART 1: General Requirements	Active
IEC	IEC 61980-/1 AMD 1 Ed. 1.0 [258]	24 July 2015	EV Wireless Power Transfer Systems—PART 1: General Requirements	Withdrawn
IEC	IEC 61980-1/COR1 [260]	25 January 2017	EV Wireless Power Transfer Systems—PART 1: General Requirements	Withdrawn

Table 11. Cont.

Standard Developer	Standard Name	Published Date	Description	Status
IEC	DRAFT IEC/TS 61980-2 Ed.1.0 [261]	11 February 2022	EV Wireless Power Transfer Systems—Part 2: Specific requirements for communication between EV and infrastructure	Active
IEC	Draft IEC/TS 61980-2 Ed. 1.0 [257]	28 August 2015	EV Wireless Power Transfer Systems—Part 3: Specific requirements for the magnetic field wireless power transfer systems	Active
IEEE	IEEE Standard C95.1 [262]	8 February 2019	IEEE Standard for Safety Levels with Respect to Human Exposure to Electric, Magnetic, and Electromagnetic Fields	Active
SAE	J2954 SAE [263]	26 August 2022	Wireless Charging of Electric and Plug-in Hybrid Vehicles	Revised
SAE	J1773 201406 [264]	5 June 2014	SAE EV Inductively Coupled Charging	Stabilized
SAE	J2847-6 [265]	29 September 2020	Communication between Wirelessly Charged Vehicles and Wireless EV Chargers	Revised
SAE	J2931-6 [266]	27 August 2015	Signaling communication for Wirelessly charged Electric Vehicle	Issued
UL	UL 2750 [204]		Outline of Investigation for Wireless Power Transfer Equipment for Electric Vehicles	Draft Released

## 8. Economic Analysis of Wireless Charging-Based Electric Vehicles

The WPT systems are competitive with other EV charging methods on three important parameters: charging infrastructure, battery, and cost of phase energy [205]. The WPT systems have only one additional device, magnetic couplers, compared with the conductive charging method. The additional material cost for the 8 kW capacity charger will be USD 400 for these couplers [105]. However, this price may be acceptable due to their improved convenience of operation.

Furthermore, WPT-based buses reduce the cost of fuel by USD 90,000 [118]. Moreover, the maintenance cost of wireless charging is much lower when compared to wired charging. There is no contact between the charger and the vehicle, so the maintenance cost of the plug will be eliminated. Batteries and Battery Management Systems (BMSs) are the most expensive part of wireless charging. If the number of charging stations is increased, the battery capacity will be reduced automatically. The battery cost function and the transmitter cost function are the two cost functions available in WPT systems. Power transmitter functions have fixed costs (inverter cost and labor cost to connect with the grid) and variable costs (depending on the airgap length). The initial cost of an EV includes the material cost of the vehicle, accessories for charging, the battery, and other factors like V2G and BMS. The main components of WPT systems are batteries, coils, and power electronics-related devices (converters and inverters). From the literature, it is clearly shown that EVs' static charging consumes less energy compared to dynamic charging. This is because dynamic charging needs to fix the continuous charging lanes on the road surface. However, it requires a small battery capacity due to instant charging. Therefore, static charging systems need to install a higher range of batteries.

The wired and wireless charging methods can be preferred for commercial and public spaces. This section focuses on the economic analysis of electric vehicles in public and private parking areas. The analysis has been done for two parking areas. They are:

- A 50 EV parking area;

- 200 EV parking garage.

The maximum cost value that the wireless charging system must exhibit to make the investment profitable is computed using traditional economic indices and considering the efficiency provided by the manufacturer companies, which are shown in Table 12.

**Table 12.** IPT characteristics.

Company	Operating Frequency [kHz]	Transferred Power [kW]	Airgap [cm]	Efficiency
WiTricity	145	3.3	18	90%
Qualcomm Halo	20	7	NA	NA
Conductix-Wampfler	NA	60–180	4	90%
Bombardier	NA	200	NA	90%
Momentum Dynamics	NA	3.3–10	61	92%
HEVO Power	85	1–10	≤30.48	≥85%

NA—Not Applicable.

The price of installing a wired or wireless charging system and the associated maintenance costs are shown in Table 13. The realization costs for a wired charging station have been calculated using a three-phase charging column that can simultaneously charge two vehicles. According to the IEC 61851-1 standard [267], the connection is Mode 2 (slow charge, 6–8 h, in alternating current with voltages up to 250 V single-phase or 480 V three-phase and 32 A maximum current), as each charging point's rated power is equal to 22 kW. The maximum current value is equal to 16 A. Both household installations and public spaces are permitted to use this mode. In this instance, the vehicle's power cable is fitted with a control box, which ensures user safety while the batteries are being charged.

The installation of a mono-phase charging point with a rated power of 7.2 kW and a rated airgap between the two coils of 10 cm has been used to calculate the realization costs for a wireless charging station [268]. The economic values listed in Table 13 show that the charging point's unusual maintenance and purchase expenses account for the largest discrepancies.

**Table 13.** Charging station rates for wireless and wired.

	Price per Pair of Charging Points [EUR]	
	Wireless	Wired
Price of the charging system's purchase	7200	3800
Initial cost of charging systems	1200	500
Additional price for maintenance/year	22	92
Price for maintenance/year	30	40

From Table 13, it has been proven that the installation cost of wireless charging is higher than that of wired charging for 7.2 kW. However, maintenance and labor costs will be higher for wired charging compared to wireless charging, and they will increase year by year. The higher rating of the cables for high-voltage transmission and sockets may economically increase the wired charging infrastructure. So, wireless charging is economical for all types of EVs, and its installation cost can be reduced further with the help of upcoming suggestions.

Regarding the high maintenance costs of wireless systems, it has been proposed to replace one charging station per 200 parking spaces annually. Even in this instance, the price has increased by 20% to account for the exceptional maintenance costs of charging stations that do not require regular repair.



Regarding the high maintenance costs of wired systems, it has been suggested that one charging column be replaced with two charging points per 50 car parking spaces annually. This price has been raised by 20% to account for the high maintenance costs of columns that do not require a complete replacement. Additionally, the typical maintenance expenses for wired and wireless systems have been examined. For both systems, the costs of routine maintenance on electric devices, components, and cables have been taken into account. Additional expenses for wired systems have also been added for partial cable and connector replacements.

The costs associated with the energy losses during transmission must be added in order to compare the costs of the two charging systems. The energy loss in the wired systems' wires will be specifically disregarded, while the wireless charging systems' inductive transfer efficiency will be considered. Aside from Tesla, which publishes values between 60 and 100 kWh [269], all full electric vehicle manufacturers install on-board battery packs with rated storage capacity between 16 and 41 kWh. The annual recharge energy values for both automobile parking typologies are shown in Table 14. A car park with 50 parking spaces will often consume between 500 and 2000 MWh annually, but a car park with 200 parking spaces will typically consume between 2000 and 20,000 MWh annually. Table 15 displays the median pricing (taxes included) for industrial consumers of electricity in Italy and Europe in 2015 for these two categories of average annual usage [270]. According to Table 15, Italy has higher electricity purchase costs than the rest of Europe.

**Table 14.** Energy recharge for each parking type for cars on an annual basis.

Availability of Parking	Number of Charges at a Point per Day	Fill Factor	Number of Days	Power [kWh]	Total Energy per Year [MWh]
50	2	0.75	300	24	540
200	2	0.7	300	24	2016

**Table 15.** Industrial energy consumption prices in Italy and Europe (in 2015).

Energy Consumption Prices [EUR/MWh]		
	Average Energy Consumption/Year 500–2000 [MWh]	Average Energy Consumption/Year 2000–20,000 [MWh]
Italy	18.64	16.62
Europe	14.86	13.23

The Net Present Value (NPV) of the expense to manage the two types of parking, assuming a lifetime for the charging systems of ten years, can be estimated in the following manner (7):

$$C_{NPV} = C_{pi} + C_{sm} + C_{om} + C_{S en} + C_{S emp} \quad (7)$$

where  $C_{NPV}$  is the net investment;  $C_{pi}$  is the initial investment;  $C_{sm}$  is the additional maintenance cost;  $C_{om}$  is the overall maintenance cost;  $C_{S en}$  is the loss of energy cost; and  $C_{S emp}$  is the charging station labor expense. The NPV of the investment cost is shown in Table 16 for both car parking typologies within the environment of the Italian market.

The NPV of the investment cost for each parking typology is shown in Table 17 within the context of the European market.

### 8.1. Economic Facilities of Static Charging

The static WPT is the most efficient and accessible form of charging in the WPT. The Korean KAIST University implemented a static WPT system that can transfer power up to 5 m with the help of dipole coil resonance. Oakridge National Labs from the USA has also tested different prototypes for static WPT [161]. Many other countries, companies,

and automotive industries like Tesla, Nissan, Qualcomm, and WiTricity are involved in developing wireless charging for EVs and ensuring that it is available for commercial purposes [162]. However, we need to concentrate more on electromagnetic emissions and coil misalignment. These two are the main drawbacks that should restrict the future adoption of commercial static WPT in EVs. In static WPT, spending some part of the budget on BMS to improve battery lifetime is mandatory. The BMS is attached to the Controller Area Network (CAN) of the EV, which controls the vehicle's sensors by using radio signals. Therefore, the overall static WPT system works automatically. There is no need for any human interaction. All charging payments can also be made with the help of advanced control and automation systems connected with BMS and CAN. WPT techniques only improve the commercial usage of EV economically. Remarkably static WPT can achieve the target of charging with less cost.

**Table 16.** In the Italian market, the NPV of the investment cost for each parking typology.

	50 EV Parking Area			200 EV Parking Area		
	Wireless (Efficiency of 0.85)	Wireless (Efficiency of 0.92)	Wired	Wireless (Efficiency of 0.85)	Wireless (Efficiency of 0.92)	Wired
$C_{pi}$ (EUR)	210	210	107,500	840	840	430
$C_{sm}$ (EUR)	8372	8372	35,008	33,486	33,486	140,033
$C_{om}$ (EUR)	5708	5708	7610	22,831	22,831	30,442
$C_{Sen}$ (EUR)	140,816	69,388	0	468,742	230,974	0
$C_{Semp}$ (EUR)	0	0	210,658	0	0	421,315
$C_{NPV}$ (EUR)	364,895	293,467	360,776	1,365,059	1,127,292	1,021,790

**Table 17.** In the European market, the NPV of the investment cost for each parking typology.

	50 EV Parking Area			200 EV Parking Area		
	Wireless (Efficiency of 0.85)	Wireless (Efficiency of 0.92)	Wired	Wireless (Efficiency of 0.85)	Wireless (Efficiency of 0.92)	Wired
$C_{pi}$ (EUR)	210	210	107,500	840	840	430
$C_{sm}$ (EUR)	8372	8372	35,008	33,486	33,486	140,033
$C_{om}$ (EUR)	5708	5708	7610	22,831	22,831	30,442
$C_{Sen}$ (EUR)	112,260	55,316	0	373,132	183,862	0
$C_{Semp}$ (EUR)	0	0	189,592	0	0	379,184
$C_{NPV}$ (EUR)	336,339	279,396	339,710	1,269,450	1,080,180	979,658

## 8.2. Economic Facilities of Dynamic Charging

The dynamic WPT technique also has advantages over other EV charging methods. Dynamic WPT can easily be implemented in highways, toll plazas, large research institutions, the automotive industry, traffic signals, etc., but installing the charging pads requires a large area. It will consume an excess amount for placing continuous charging pads on the road. Instead of that, it will not require any higher-range batteries. So, a dynamic WPT manages the economic cost of battery capacity. Jeong et al. discussed mathematical optimization techniques for battery size in dynamic WPT and compared the total cost of static and dynamic WPT systems. This comparison study has been conducted on the

18 EVs for ten years. This study concludes that USD 2,462,268 was the cost of the difference in total cost for static and dynamic charging technique implementations. It costs 20.8% less to implement the dynamic WPT system. Dynamic WPT requires a large area for installing charging pads with a lower battery capacity range [206].

The quasi-dynamic WPT technique charges the EV battery at a standstill position at bus stops, consuming the power within a few minutes. Thus, quasi-dynamic WPT will reduce the number of charging lanes and the cost of batteries. In addition, it can improve the ability to charge the battery by using fast-charging techniques at bus stops within a few minutes. The United Kingdom (UK) introduced and tested the quasi-dynamic WPT for commercial use. Furthermore, researchers and industries are working to implement this technique on highways [190].

## 9. Conclusions and Future Scope

This substantial literature study presents an extensive review of various EV charging technologies and outlines conventional conductive charging and its merits and demerits. The principle of wireless charging and its coil design are discussed in detail. Further, the factors influencing the WPT are discussed. In continuation, the efficiency enhancement of wireless charging technologies, including compensation topologies and misalignment mitigation techniques, is also discussed in detail.

This study identifies notable challenges and research gaps in WPT systems. To achieve maximum efficiency in the WPT system, researchers shall focus on misalignment problems, airgap optimization, coil shape, and design. The open challenges in dynamic charging systems are explicated from the perspective of system efficiency, speed, range, and battery life span. WPT advancement will get an essential part of electrification in the transportation application once the above challenges are unraveled.

There are different shapes of coil designs, and types of compensation topologies have been studied for varying power levels in EV applications. Therefore, suggesting that a particular type is suitable for another is pretty challenging. However, the review presents different coil shapes and compensation topologies in Table 7 and Section 6, respectively. Predominantly, the triple quadrature coil with double-sided LCC and LCC-SS combinational compensation topologies gives more efficiency than other structures, as shown in Tables 9 and 10. Thus, researchers can select the appropriate design and topology for their required applications and attain better efficiency.

The efficiency and dependability of WPT have increased due to technological advancements. This has made it more useful for usage in various applications, such as electric vehicles and industrial automation. WPT has expanded due to the introduction of Internet of Things (IoT) devices in EVs. Wireless charging is a practical and effective technique to offer the continuous power these devices need. Research and development expenditures for WPT technology have increased significantly. As a result, fresh and cutting-edge applications have been created, and it is anticipated that this will spur more growth in the future. Overall, technical improvements, rising demand for mobile devices, and expanding acceptance in various industries are projected to fuel the trend of wireless power transfer in the upcoming years.

**Author Contributions:** Analysis, writing—original draft preparation, and investigation, B.A.R.; conceptualization, validation, writing—review, editing, analysis, and supervision, U.S. and S.B. All authors have read and agreed to the published version of the manuscript.

**Funding:** This research received no external funding.

**Data Availability Statement:** Not applicable.

**Acknowledgments:** We gratefully acknowledge the faculties from the School of Electrical Engineering, VIT, Vellore for providing the inputs and suggestions to improve the paper. Also, the authors would like to thank Renewable Energy Lab, Prince Sultan University for their support and guidance.

**Conflicts of Interest:** The authors declare no conflict of interest.

### Abbreviations

EV	Electric Vehicle
ICE	Internal Combustion Engine
DC	Direct Current
USA	United States of America
WPT	Wireless Power Transfer
V2G	Vehicle to Grid
G2V	Grid to Vehicle
AC	Alternating Current
ZVS	Zero Voltage Switching
ZCS	Zero Current Switching
LC	Inductor-Capacitor
EMI	Electromagnetic Interference
PHEV	Plug-in Hybrid Electric Vehicles
Hr	Hour
kWh	Kilowatt Hour
cm	Centimeter
Km	Kilometer
€	Euro
Li-Ion	Lithium Ion
Na – NiCl <sub>2</sub>	Sodium Nickel Chloride
Ni-MH	Nickel Metal Hydride
Li-S	Lithium Sulfur
Kg	Kilogram
SOC	State of Charge
SOH	State of Health
CCWPT	Capacitive Coupling Wireless Power Transfer
CMR	Coupled Magnetic Resonance
IPT	Inductive Power Transfer
PMC	Permanent Magnet Coupled transfer
NASA	National Aeronautics and Space Administration
PCB	Printed Circuit Board
SHARP	Stationary High-Altitude Relay Platform
$V_{IN}$	Input Voltage
$V_{OUT}$	Output Voltage
$R_L$	Load Resistance
$C_{cc}$	Capacitance
MHz	Megahertz
GHz	Gigahertz
LED	Light Emitting Diode
RFID	Radio Frequency Identification
DWC	Dynamic Wireless Charging
TULIP	Transport Urban Libre Individual Public
ORNL	Oak Ridge National Laboratory
EMF	Electromotive Force
GPSSC	Grouped Periodic Series Spiral Coupler
KAIST	Korea Advanced Institute of Science and Technology
PTS	Parity-Time Symmetric
FEA	Finite Element Analysis
PPs	Polarized Pads
NPPs	Non-Polarized Pads
DD	Double-D Coil
DDQ	Non-Polarized pad Double-D coil
DDQP	Non-Polarized pad Double-D Quadrature coil
BP	Bi-Polar
$T_o$	Quality Factor
$R_o$	Equivalent Resistance
$\omega$	Resonant Frequency

M	Mutual Inductance
SS	Series-Series
SP	Series-Parallel
PS	Parallel-Series
PP	Parallel-Parallel
SPS	Series-Parallel-Series
k	Coupling coefficient
$L_p$	Self-inductance of the primary coil
$L_s$	Self-inductance of the secondary coil
\$	Dollar
CAN	Controller Area Network
BMS	Battery Management System
SAE	Society of Automotive Engineers
IEC	International Electrotechnical Commission
ICES	International Committee on Electromagnetic Safety
IEEE	Institute of Electrical and Electronics Engineers
ICNIRP	International Commission on Non-Ionizing Radiation Protection
UL	Underwriter Laboratories

## References

- Dai, J.; Ludois, D.C. A Survey of Wireless Power Transfer and a Critical Comparison of Inductive and Capacitive Coupling for Small Gap Applications. *IEEE Trans. Power Electron.* **2015**, *30*, 6017–6029. [\[CrossRef\]](#)
- Pathipati, V.K. *Design of a Novel Ferrite Core-based Highly Efficient Wireless Resonant Inductive Power Transfer System*; University of Ontario Institute of Technology: Oshawa, ON, USA, 2016.
- Miller, J.M.; Onar, O.C.; Chinthavali, M. Primary-side power flow control of wireless power transfer for electric vehicle charging. *IEEE J. Emerg. Sel. Top. Power Electron.* **2015**, *3*, 147–162. [\[CrossRef\]](#)
- Qiu, C.; Chau, K.T.; Liu, C.; Chan, C.C. Overview of wireless power transfer for electric vehicle charging. In Proceedings of the 2013 World Electric Vehicle Symposium and Exhibition (EVS27), Barcelona, Spain, 17–20 November 2014; pp. 1–9.
- Sasaki, S.; Tanaka, K.; Maki, K.I. Microwave power transmission technologies for solar power satellites. *Proc. IEEE* **2013**, *101*, 1438–1447. [\[CrossRef\]](#)
- Choi, S.Y.; Gu, B.W.; Jeong, S.Y.; Rim, C.T. Advances in wireless power transfer systems for roadway-powered electric vehicles. *IEEE J. Emerg. Sel. Top. Power Electron.* **2015**, *3*, 18–36. [\[CrossRef\]](#)
- Mi, C.C.; Buja, G.; Choi, S.Y.; Rim, C.T. Modern Advances in Wireless Power Transfer Systems for Roadway Powered Electric Vehicles. *IEEE Trans. Ind. Electron.* **2016**, *63*, 6533–6545. [\[CrossRef\]](#)
- Ahmad, F.; Alam, M.S.; Asaad, M. Developments in xEVs charging infrastructure and energy management system for smart microgrids including xEVs. *Sustain. Cities Soc.* **2017**, *35*, 552–564. [\[CrossRef\]](#)
- Wang, H.; Fan, Y.; Chen, C.; Tao, T.; Qiao, Z. Novel estimation solution on lithium-ion battery state of charge with current-free detection algorithm. *IET Circuits Devices Syst.* **2019**, *13*, 245–249. [\[CrossRef\]](#)
- Tesla, N. Apparatus for Transmitting Electrical Energy. U.S. Patent 1,119,732, 12 December 1914.
- Chen, L.; Liu, S.; Zhou, Y.C.; Cui, T.J. An optimizable circuit structure for high-efficiency wireless power transfer. *IEEE Trans. Ind. Electron.* **2013**, *60*, 339–349. [\[CrossRef\]](#)
- Li, S.; Liu, Z.; Zhao, H.; Zhu, L.; Shuai, C.; Chen, Z. Wireless Power Transfer by Electric Field Resonance and Its Application in Dynamic Charging. *IEEE Trans. Ind. Electron.* **2016**, *63*, 6602–6612. [\[CrossRef\]](#)
- Esmaili Jamakani, B.; Mosallanejad, A.; Afjei, E.; Lahooti Eshkevari, A. Investigation of triple quadrature pad for wireless power transfer system of electric vehicles. *IET Electr. Syst. Transp.* **2020**, *11*, 58–68. [\[CrossRef\]](#)
- Nguyen, H.N.T.; Zhang, C.; Mahmud, M.A. Optimal Coordination of G2V and V2G to Support Power Grids with High Penetration of Renewable Energy. *IEEE Trans. Transp. Electrif.* **2015**, *1*, 188–195. [\[CrossRef\]](#)
- Wireless Chargers Archives—Qi Wireless Charging. Available online: <http://www.qiwireless.com/category/wirelesschargers/> (accessed on 29 August 2022).
- Barnard, J.M.; Ferreira, J.A.; Van Wyk, J.D. Sliding transformers for linear contactless power delivery. *IEEE Trans. Ind. Electron.* **1997**, *44*, 774–779. [\[CrossRef\]](#)
- Coloma, P.; Donini, A.; Migliozi, P.; Lavina, L.S.; Terranova, F. A High Efficiency 3.3 kW Loosely-Coupled Wireless Power Transfer System without Magnetic Material. *AIP Conf. Proc.* **2011**, *1382*, 262–264.
- Dik, A.; Omer, S.; Boukhanouf, R. Electric Vehicles: V2G for Rapid, Safe, and Green EV Penetration. *Energies* **2022**, *15*, 803. [\[CrossRef\]](#)
- Jain, P.; Jain, T. Impacts of G2V and V2G power on electricity demand profile. In Proceedings of the 2014 IEEE International Electric Vehicle Conference (IEVC), Florence, Italy, 17–19 December 2014.
- Huang, X.; Qiang, H.; Huang, Z.; Sun, Y.; Li, J. The interaction research of smart grid and EV based wireless charging. In Proceedings of the IEEE Vehicle Power and Propulsion Conference, Gijón, Spain, 26–29 October 2013; pp. 354–358.

21. Habib, S.; Kamran, M.; Rashid, U. Impact analysis of vehicle-to-grid technology and charging strategies of electric vehicles on distribution networks—A review. *J. Power Sources* **2015**, *277*, 205–214. [CrossRef]
22. Cheng, A.J.; Tarroja, B.; Shaffer, B.; Samuelson, S. Comparing the emissions benefits of centralized vs. decentralized electric vehicle smart charging approaches: A case study of the year 2030 California electric grid. *J. Power Sources* **2018**, *401*, 175–185. [CrossRef]
23. Tan, K.M.; Ramachandaramurthy, V.K.; Yong, J.Y. Integration of electric vehicles in smart grid: A review on vehicle to grid technologies and optimization techniques. *Renew. Sustain. Energy Rev.* **2016**, *53*, 720–732. [CrossRef]
24. Ahmad, A.; Khan, Z.A.; Saad Alam, M.; Khateeb, S. A Review of the Electric Vehicle Charging Techniques, Standards, Progression, and Evolution of EV Technologies in Germany. *Smart Sci.* **2018**, *6*, 36–53. [CrossRef]
25. Gschwendtner, C.; Sinsel, S.R.; Stephan, A. Vehicle-to-X (V2X) implementation: An overview of predominate trial configurations and technical, social and regulatory challenges. *Renew. Sustain. Energy Rev.* **2021**, *145*, 110977. [CrossRef]
26. Erdinc, O.; Tascikaraoglu, A.; Paterakis, N.G.; Dursun, I.; Sinim, M.C.; Catalao, J.P.S. Comprehensive Optimization Model for Sizing and Siting of DG Units, EV Charging Stations, and Energy Storage Systems. *IEEE Trans. Smart Grid.* **2018**, *9*, 3871–3882. [CrossRef]
27. Li, T.; Zhang, J.; Zhang, Y.; Jiang, L.; Li, B.; Yan, D.; Ma, C. An optimal design and analysis of a hybrid power charging station for electric vehicles considering uncertainties. In Proceedings of the IECON 2018—44th Annual Conference of the IEEE Industrial Electronics Society, Washington, DC, USA, 21–23 October 2018; Volume 1, pp. 5147–5152.
28. Fathabadi, H. Novel grid-connected solar/wind powered electric vehicle charging station with vehicle-to-grid technology. *Energy* **2017**, *132*, 1–11. [CrossRef]
29. Sufyan, M.; Rahim, N.A.; Muhammad, M.A.; Tan, C.K.; Raihan, S.R.S.; Bakar, A.H.A. Charge coordination and battery lifecycle analysis of electric vehicles with V2G implementation. *Electr. Power Syst. Res.* **2020**, *184*, 106307. [CrossRef]
30. Hui, S.Y.R.; Zhong, W.; Lee, C.K. A critical review of recent progress in mid-range wireless power transfer. *IEEE Trans. Power Electron.* **2013**, *29*, 4500–4511. [CrossRef]
31. Machura, P.; Li, Q. A critical review on wireless charging for electric vehicles. *Renew. Sustain. Energy Rev.* **2019**, *104*, 209–234. [CrossRef]
32. Manohar, B.S.P.S.; Gandham, V.V.S.K.; Dhal, P.K. An Overview of Wireless Power Transmission System and Analysis of Different Methods. *Int. J. Res. Appl. Sci. Eng. Technol.* **2022**, *3*, 1818–1827. [CrossRef]
33. Aydin, E.; Aydemir, M.T.; Aksoz, A.; El Baghdadi, M.; Hegazy, O. Inductive Power Transfer for Electric Vehicle Charging Applications: A Comprehensive Review. *Energies* **2022**, *15*, 4962. [CrossRef]
34. Will DC Fast Charging Harm Electric Car Batteries? Available online: <https://www.cnet.com/roadshow/news/will-dc-fast-charging-harm-electric-car-batteries/> (accessed on 23 August 2022).
35. EV DC—DC Fast Chargers. Available online: <https://www.power-sonic.com/dc-fast-chargers/> (accessed on 31 January 2023).
36. Lukic, S.; Pantic, Z. Cutting the Cord: Static and Dynamic Inductive Wireless Charging of Electric Vehicles. *IEEE Electr. Mag.* **2013**, *1*, 57–64. [CrossRef]
37. Ahmadian, A.; Mohammadi-Ivatloo, B.; Elkamel, A. A Review on Plug-in Electric Vehicles: Introduction, Current Status, and Load Modeling Techniques. *J. Mod. Power Syst. Clean Energy* **2020**, *8*, 412–425. [CrossRef]
38. Yilmaz, M.; Krein, P.T. Review of battery charger topologies, charging power levels, and infrastructure for plug-in electric and hybrid vehicles. *IEEE Trans. Power Electron.* **2013**, *28*, 2151–2169. [CrossRef]
39. Mude, K.N. Battery charging method for electric vehicles: From wired to on-road wireless charging, Chinese. *J. Electr. Eng.* **2018**, *4*, 1–15. [CrossRef]
40. Khaligh, A.; Dusmez, S. Comprehensive topological analysis of conductive and inductive charging solutions for plug-in electric vehicles. *IEEE Trans. Veh. Technol.* **2012**, *61*, 3475–3489. [CrossRef]
41. J1772: SAE Electric Vehicle and Plug-in Hybrid Electric Vehicle Conductive Charge Coupler—SAE International. Available online: [http://standards.sae.org/j1772\\_201602/](http://standards.sae.org/j1772_201602/) (accessed on 23 August 2022).
42. Veneri, O.; Ferraro, L.; Capasso, C.; Iannuzzi, D. Charging infrastructures for EV: Overview of technologies and issues. In Proceedings of the 2012 Electrical Systems for Aircraft, Railway and Ship Propulsion, Bologna, Italy, 16–18 November 2012.
43. PluginCars.com. Porsche Panamera S. E-Hybrid Review. Available online: <http://www.pluginCars.com/porsche-panamera-s-e-hybrid> (accessed on 21 September 2022).
44. Audi A3 Sportback e-tron. Available online: <https://www.audiusa.com/models/audi-a3-sportback-e-tron/> (accessed on 21 September 2022).
45. Specs Cadillac ELR Forum. Available online: <https://www.gm-volt.com/threads/review-2014-cadillac-elr.337369/> (accessed on 21 September 2022).
46. Chevrolet Pressroom-United States—Spark EV. Available online: <http://media.chevrolet.com/media/us/en/chevrolet/vehicles/spark-ev/2016.tab1.html> (accessed on 26 September 2022).
47. Ford C-MAX Energi SE Plug-in Hybrid Model Highlights Ford. Com. Available online: <https://www.ford.com/cars/c-max/2017/models/c-max-energi-se/> (accessed on 22 September 2022).
48. Mercedes S550 Plug-in Hybrid | PluginCars.Com. Available online: <http://www.pluginCars.com/mercedes-s550-plug-hybrid> (accessed on 22 September 2022).

49. Mercedes-Benz C350 Plug-in Hybrid—EVBox. Available online: <https://evchargeplus.com/ev-specification/mercedes-benz-c350-plug-in-hybrid/> (accessed on 26 September 2022).
50. Smart Electric Drive | PluginCars.Com. Available online: <http://www.pluginCars.com/smart-ed> (accessed on 26 September 2022).
51. The Toyota Prius Plug-in Hybrid | PluginCars.Com. Available online: <http://pluginCars.com/toyota-prius-plugin-hybrid> (accessed on 26 September 2022).
52. Specifications i-MiEV MITSUBISHI MOTORS. Available online: <http://www.mitsubishi-motors.com/en/showroom/i-miev/specifications/> (accessed on 26 September 2022).
53. Nissan LEAF Will Include Fast Charge Capability and Emergency Charging Cable at Launch—Gas 2. Available online: <https://www.zap-map.com/charge-points/nissan-leaf-2430kwh-charging-guide/> (accessed on 26 September 2022).
54. Review and Pictures of Porsche Cayenne S E-Hybrid | PluginCars.Com. Available online: <http://www.pluginCars.com/porsche-cayenne-s-e-hybrid> (accessed on 26 September 2022).
55. Volkswagen e-Golf Specifications. Available online: <http://www.neftinvw.com/blog/2017-volkswagen-e-golf-specifications/> (accessed on 26 September 2022).
56. Specs Ford Focus Electric Forum, My Focus Electric. Available online: <http://www.myfocuselectric.com/specs/> (accessed on 26 September 2022).
57. Fiat 500e | PluginCars.Com. Available online: <http://www.pluginCars.com/fiat-500e> (accessed on 26 September 2022).
58. Kia Soul EV Specifications. Available online: <http://www.kiamedia.com/us/en/models/soul-ev/2017/specifications> (accessed on 26 September 2022).
59. Honda Accord Plug-in Hybrid | PluginCars.Com. Available online: <http://www.pluginCars.com/honda-accord-plug-hybrid> (accessed on 26 September 2022).
60. BMW i3 (94 Ah) Release Date, Price and Specs—Roadshow. Available online: <https://www.cnet.com/roadshow/auto/2017-bmw-i3/preview/> (accessed on 26 September 2022).
61. Mercedes B—Class Electric (Pure EV). Available online: <https://www.mercedes-benz.com/en/vehicles/passenger-cars/b-class/> (accessed on 26 September 2022).
62. Tesla Model S (Pure EV). Available online: <https://www.tesla.com/blog/new-tesla-model-s-now-quickest-production-car-world> (accessed on 26 September 2022).
63. Iclodean, C.; Varga, B.; Burnete, N.; Cimerdean, D.; Jurchiş, B. Comparison of Different Battery Types for Electric Vehicles. *IOP Conf. Ser. Mater. Sci. Eng.* **2017**, *252*, 012058. [CrossRef]
64. EV Charging Standards and Specifications. Available online: <https://electrek.co/2021/07/21/electric-vehicle-ev-charging-standards-and-how-they-differ/> (accessed on 17 October 2022).
65. EV Dc Fast Charging Standards. Available online: <https://greentransportation.info/ev-charging/range-confidence/chap8-tech/ev-dc-fast-charging-standards-chademo-ccs-sae-combo-tesla-supercharger-etc.html> (accessed on 17 October 2022).
66. Duan, C.; Jiang, C.; Taylor, A.; Bai, K.H. Design of a zero-voltage-switching large-air-gap wireless charger with low electric stress for electric vehicles. *IET Power Electron.* **2013**, *6*, 1742–1750. [CrossRef]
67. Ahmad, A.; Alam, M.S.; Chaban, R.C. Efficiency enhancement of wireless charging for Electric vehicles through reduction of coil misalignment. In Proceedings of the 2017 IEEE Transportation Electrification Conference and Expo (ITEC), Chicago, IL, USA, 22–24 June 2017; pp. 21–26.
68. Chen, W.; Liu, C.; Lee, C.H.T.; Shan, Z. Cost-effectiveness comparison of coupler designs of wireless power transfer for electric vehicle dynamic charging. *Energies* **2016**, *9*, 906. [CrossRef]
69. Buja, G.; Chun-Taek, R.; Chunting, C. Mi, Dynamic charging for electric vehicles (EV) by wireless power transfer. *IEEE Trans. Ind. Electron.* **2016**, *63*, 6530–6532. [CrossRef]
70. Bhattacharya, S.; Tan, Y.K. Design of static wireless charging coils for integration into electric vehicle. In Proceedings of the 2012 IEEE Third International Conference on Sustainable Energy Technologies (ICSET), Kathmandu, Nepal, 24–27 September 2012; pp. 146–151.
71. Vukajlovic, N.; Milićević, D.; Dumnic, B.; Popadic, B. Comparative analysis of the supercapacitor influence on lithium battery cycle life in electric vehicle energy storage. *J. Energy Storage* **2020**, *31*, 101603. [CrossRef]
72. Li, Z.; Zhu, C.; Jiang, J.; Song, K.; Wei, G. A 3-kW Wireless Power Transfer System for Sightseeing Car Supercapacitor Charge. *IEEE Trans. Power Electron.* **2017**, *32*, 3301–3316. [CrossRef]
73. Elahi, A.; Amin, A.A.; Shami, U.T.; Usman, M.T.; Iqbal, M.S. Efficient wireless charging system for supercapacitor-based electric vehicle using inductive coupling power transfer technique. *Adv. Mech. Eng.* **2019**, *11*, 1–10. [CrossRef]
74. Wang, R.; Yao, M.; Niu, Z. Smart supercapacitors from materials to devices. *InfoMat* **2020**, *2*, 113–125. [CrossRef]
75. Sudworth, J.L. The sodium/nickel chloride (ZEBRA) battery. *J. Power Sources* **2001**, *100*, 149–163. [CrossRef]
76. Hawkins, T.R.; Singh, B.; Majeau-Bettez, G.; Strømman, A.H. Comparative Environmental Life Cycle Assessment of Conventional and Electric Vehicles. *J. Ind. Ecol.* **2013**, *17*, 53–64. [CrossRef]
77. Nykvist, B.; Nilsson, M. Rapidly falling costs of battery packs for electric vehicles. *Nat. Clim. Chang.* **2015**, *5*, 329–332. [CrossRef]
78. Chen, Z.; Guo, N.; Li, X.; Shen, J.; Xiao, R.; Li, S. Battery pack grouping and capacity improvement for electric vehicles based on a genetic algorithm. *Energies* **2017**, *10*, 439. [CrossRef]
79. Gerssen-Gondelach, S.J.; Faaij, A.P.C. Performance of batteries for electric vehicles on short and longer term. *J. Power Sources* **2012**, *212*, 111–129. [CrossRef]

80. Budde-Meiwes, H.; Drillkens, J.; Lunz, B.; Muennix, J.; Rothgang, S.; Kowal, J.; Sauer, D.U. A review of current automotive battery technology and future prospects. *Proc. Inst. Mech. Eng. Part D J. Automob. Eng.* **2013**, *227*, 761–776. [[CrossRef](#)]
81. Doughty, D.; Roth, E.P. A General Discussion of Li Ion Battery Safety. *Electrochem. Soc. Interface* **2012**, *21*, 37–44.
82. Ji, D.; Chen, L.; Ma, T.; Wang, J.; Liu, S.; Ma, X.; Wang, F. Research on adaptability of charging strategy for electric vehicle power battery. *J. Power Sources* **2019**, *437*, 1–9. [[CrossRef](#)]
83. Salgado, R.M.; Danzi, F.; Oliveira, J.E.; El-Azab, A.; Camanho, P.P.; Braga, M.H. The Latest Trends in Electric Vehicles Batteries. *Molecules* **2021**, *26*, 3188. [[CrossRef](#)]
84. Lu, L.; Han, X.; Li, J.; Hua, J.; Ouyang, M. A review on the key issues for lithium-ion battery management in electric vehicles. *J. Power Sources* **2013**, *226*, 272–288. [[CrossRef](#)]
85. Zou, Y.; Hu, X.; Ma, H.; Li, S.E. Combined State of Charge and State of Health estimation over lithium-ion battery cell cycle lifespan for electric vehicles. *J. Power Sources* **2015**, *273*, 793–803. [[CrossRef](#)]
86. Wang, K.; Wang, W.; Wang, L.; Li, L. An improved SOC control strategy for electric vehicle hybrid energy storage systems. *Energies* **2020**, *13*, 5297. [[CrossRef](#)]
87. Wang, K.; Liu, C.; Sun, J.; Zhao, K.; Wang, L.; Song, L.; Duan, C.; Li, L. State of Charge Estimation of Composite Energy Storage Systems with Supercapacitors and Lithium Batteries. *Complexity* **2021**, *2021*, 8816250. [[CrossRef](#)]
88. Thounthong, P.; Raël, S.; Davat, B. Energy management of fuel cell/battery/supercapacitor hybrid power source for vehicle applications. *J. Power Sources* **2009**, *193*, 376–385. [[CrossRef](#)]
89. Omariba, Z.B.; Zhang, L.; Sun, D. Review of Battery Cell Balancing Methodologies for Optimizing Battery Pack Performance in Electric Vehicles. *IEEE Access* **2019**, *7*, 129335–129352. [[CrossRef](#)]
90. Choi, S.; Huh, J.; Lee, W.Y.; Lee, S.W.; Rim, C.T. New cross-segmented power supply rails for roadway-powered electric vehicles. *IEEE Trans. Power Electron.* **2013**, *28*, 5832–5841. [[CrossRef](#)]
91. Budhia, M.; Boys, J.T.; Covic, G.A.; Huang, C.Y. Development of a single-sided flux magnetic coupler for electric vehicle IPT charging systems. *IEEE Trans. Ind. Electron.* **2013**, *60*, 318–328. [[CrossRef](#)]
92. Miller, J.M.; Jones, P.T.; Li, J.M.; Onar, O.C. ORNL experience and challenges facing dynamic wireless power charging of EV's. *IEEE Circuits Syst. Mag.* **2015**, *15*, 40–53. [[CrossRef](#)]
93. Ojika, S.; Miura, Y.; Ise, T. Evaluation of Inductive Contactless Power Transfer Outlet with Coaxial Coreless Transformer. *Electr. Eng. Japan* **2016**, *195*, 57–67. [[CrossRef](#)]
94. Jiang, A.; Maglaras, F.V.; Moschoyiannis, S. Dynamic wireless charging of electric vehicles on the move with Mobile Energy Disseminators. *Int. J. Adv. Comput. Sci. Appl.* **2015**, *6*, 1–13.
95. Mohamed, A.A.S.; Lashway, C.R.; Mohammed, O. Modeling and feasibility analysis of quasi-dynamic WPT system for EV applications. *IEEE Trans. Transp. Electrification* **2017**, *3*, 343–353. [[CrossRef](#)]
96. Garnica, J.; Chinga, R.A.; Lin, J. Wireless power transmission: From far field to near field. *Proc. IEEE* **2013**, *101*, 1321–1331. [[CrossRef](#)]
97. Brown, W.C. The History of Power Transmission by Radio Waves. *IEEE Trans. Microw. Theory Tech.* **1984**, *32*, 1230–1242. [[CrossRef](#)]
98. Hiroshi, M. Research on Solar Power Satellites and Microwave Power Transmission in Japan. *Earth* **2002**, *3*, 36–45.
99. Brown, W.C. The history of wireless power transmission. *Sol. Energy* **1996**, *56*, 3–21. [[CrossRef](#)]
100. Zhu, X.; Jin, K.; Hui, Q.; Gong, W.; Mao, D. Long-Range Wireless Microwave Power Transmission: A Review of Recent Progress. *IEEE J. Emerg. Sel. Top. Power Electron.* **2021**, *9*, 4932–4946. [[CrossRef](#)]
101. Scharfman, W.E.; Taylor, W.C.; Morita, T. Breakdown Limitations on the Transmission of Microwave Power through the Atmosphere. *IEEE Trans. Antennas Propag.* **1964**, *12*, 709–717. [[CrossRef](#)]
102. Jin, K.; Zhou, W. Wireless Laser Power Transmission: A Review of Recent Progress. *IEEE Trans. Power Electron.* **2019**, *34*, 3842–3859. [[CrossRef](#)]
103. Mahmood, A.; Ismail, A.; Zaman, Z.; Fakhar, H.; Najam, Z.; Hasan, M.S.; Ahmed, S.H. A Comparative Study of Wireless Power Transmission Techniques. *J. Basic Appl. Sci. Res.* **2014**, *4*, 321–326.
104. Kapranov, V.V.; Matsak, I.S.; Tugaenko, V.Y.; Blank, A.V.; Suhareva, N.A. Atmospheric turbulence effects on the performance of the laser wireless power transfer system, Free. *Laser Commun. Atmos. Propag.* **2017**, *10096*, 100961E.
105. Umenei, A.E. *Understanding Low Frequency Non-Radiative Power Transfer*; Fulton Innovations White Papers; Fulton Innovation: Ada, MI, USA, 2011.
106. Sazonov, E. *Wearable Sensors*, 2nd ed.; Elsevier: Amsterdam, The Netherlands, 2021.
107. Sun, Z.; Xie, T.; Wang, X. *Wireless Power Transfer for Medical Microsystems*; Springer: New York, NY, USA, 2013.
108. Chabalko, M.J.; Besnoff, J.; Ricketts, D.S. Magnetic Field Enhancement in Wireless Power with Metamaterials and Magnetic Resonant Couplers. *IEEE Antennas Wirel. Propag. Lett* **2016**, *15*, 452–455. [[CrossRef](#)]
109. Agbinya, J.I. *Wireless Power Transfer*; River Publishers: Aalborg, Denmark, 2016.
110. Huang, L.; Hu, A.P.; Swain, A.; Kim, S.; Ren, Y. An overview of capacitively coupled power transfer—A new contactless power transfer solution. In Proceedings of the 2013 IEEE 8th Conference on Industrial Electronics and Applications, Melbourne, VIC, Australia, 19–21 June 2013; pp. 461–465.
111. Andreou, A.G. Capacitive Inter-Chip Data and Power Transfer for 3-D VLSI, *IEEE Trans. Circuits Syst. II Express Briefs* **2006**, *53*, 1348–1352.



112. Sodagar, A.M.; Amiri, P. Capacitive coupling for power and data telemetry to implantable biomedical microsystems. In Proceedings of the 4th International IEEE/EMBS Conference on Neural Engineering, Antalya, Turkey, 29 April–2 May 2009; pp. 411–414.
113. Jegadeesan, R.; Agarwal, K.; Guo, Y.X.; Yen, S.C.; Thakor, N.V. Wireless Power Delivery to Flexible Subcutaneous Implants Using Capacitive Coupling. *IEEE Trans. Microw. Theory Tech.* **2017**, *65*, 280–292. [CrossRef]
114. Shmilovitz, D.; Abramovitz, A.; Reichman, I. Quasi-Resonant LED Driver with Capacitive Isolation and High PF. In Proceedings of the 2014 IEEE Applied Power Electronics Conference and Exposition—APEC 2014, Fort Worth, TX, USA, 16–20 March 2015; Volume 3, pp. 633–641.
115. Wang, K.; Sanders, S. Contactless USB—A capacitive power and bidirectional data transfer system. In Proceedings of the 2014 IEEE Applied Power Electronics Conference and Exposition—APEC 2014, Fort Worth, TX, USA, 16–20 March 2014; pp. 1342–1347.
116. Mostafa, T.M.; Muharam, A.; Hattori, R. Wireless battery charging system for drones via capacitive power transfer. In Proceedings of the 2017 IEEE PELS Workshop on Emerging Technologies: Wireless Power Transfer (WoW), Chongqing, China, 20–22 May 2017; pp. 1–6.
117. Kurs, A.; Karalis, A.; Moffatt, R.; Joannopoulos, J.D.; Fisher, P.; Soljacic, M. Wireless power transfer via strongly coupled magnetic resonances. *Science* **2007**, *317*, 83–86. [CrossRef]
118. World’s First Road-Powered Electric Vehicle Network Switches on in South Korea—ExtremeTech. Available online: <https://www.extremetech.com/extreme/163171-worlds-first-road-powered-electric-vehicle-network-switches-on-in-south-korea> (accessed on 12 August 2022).
119. Shin, J.; Shin, S.; Kim, Y.; Ahn, S.; Lee, S.; Jung, G.; Jeon, S.J.; Cho, D.H. Design and implementation of shaped magnetic-resonance-based wireless power transfer system for roadway-powered moving electric vehicles. *IEEE Trans. Ind. Electron.* **2014**, *61*, 1179–1192. [CrossRef]
120. Ahn, S.; Lee, J.Y.; Cho, D.H.; Kim, J. Magnetic field design for low emf and high efficiency wireless power transfer system in on-line electric vehicles. In Proceedings of the 21st CIRP Design Conference Korea 2011: Interdisciplinary Design, Daejeon, Republic of Korea, 30–31 March 2011; pp. 233–239.
121. Imura, T.; Okabe, H.; Uchida, T.; Hori, Y. Study on open and short end helical antennas with capacitor in series of wireless power transfer using magnetic resonant couplings. In Proceedings of the 2009 35th Annual Conference of IEEE Industrial Electronics, Porto, Portugal, 3–5 November 2009; pp. 3848–3853.
122. Mizuno, T.; Yachi, S.; Kamiya, A.; Yamamoto, D. Improvement in efficiency of wireless power transfer of magnetic resonant coupling using magnetoplated wire. *IEEE Trans. Magn.* **2011**, *47*, 4445–4448. [CrossRef]
123. Li, W. *High-Efficiency Wireless Power Transmission at Low Frequency Using Permanent Magnet Coupling*; University of British Columbia: Vancouver, BC, Canada, 2009.
124. Covic, G.A.; Boys, J.T.; Budhia, M.; Huang, C.Y. Electric vehicles—personal transportation for the future. *World Electr. Veh. J.* **2011**, *4*, 693–704. [CrossRef]
125. Musavi, F.; Edington, M.; Eberle, W. Wireless power transfer: A survey of EV battery charging technologies. *IEEE Energy Convers. Congr. Expo. ECCE* **2012**, 1804–1810.
126. Bosshard, R.; Kolar, J.W. Multi-Objective Optimization of C/85 kHz IPT System for Public Transport. *IEEE J. Emerg. Sel. Top. Power Electron.* **2016**, *4*, 1370–1382. [CrossRef]
127. Budhia, M.; Covic, G.; Boys, J. A new IPT magnetic coupler for electric vehicle charging systems. In Proceedings of the IECON 2010—36th Annual Conference on IEEE Industrial Electronics Society, Glendale, AZ, USA, 7–10 November 2010; pp. 2487–2492.
128. Nagendra, G.R.; Covic, G.A.; Boys, J.T. Determining the physical size of inductive couplers for IPT EV systems. *IEEE J. Emerg. Sel. Top. Power Electron.* **2014**, *3*, 571–583. [CrossRef]
129. Dashora, H.K.; Bertoluzzo, M.; Buja, G. Reflexive properties for different pick-up circuit topologies in a distributed IPT track. In Proceedings of the 2015 IEEE 13th International Conference on Industrial Informatics (INDIN), Cambridge, UK, 22–24 July 2015; pp. 69–75.
130. Kazmierkowski, M.P.; Moradewicz, A.J. Unplugged but connected: Review of contactless energy transfer systems. *IEEE Ind. Electron. Mag.* **2012**, *6*, 47–55. [CrossRef]
131. Oersted, H.C. Experiments on the effect of a current of electricity on the magnetic needle. *Matrix Tensor Q.* **1981**, *32*, 60–62.
132. Maxwell, J.C. Summary for policymakers. *Treatise Electr. Magn.* **1954**, *53*, 1–30.
133. Ampere’s Law—Reference Notes. Available online: <http://notes.tyrocity.com/ampere-law/> (accessed on 18 August 2022).
134. Lopez-Ramos, A.; Menendez, J.R.; Pique, C. Conditions for the validity of Faraday’s law of induction and their experimental confirmation. *Eur. J. Phys.* **2008**, *29*, 1069–1076. [CrossRef]
135. Justin. A. Biot–Savart law. *Int. J. Res.* **2015**, *2*, 2348–6848.
136. Maxwell, J.C. A dynamical theory of the electromagnetic field. *R. Soc.* **2012**, *2*, 32.
137. Lu, X.; Wang, P.; Niyato, D.; Kim, D.I.; Han, Z. Wireless Charging Technologies: Fundamentals, Standards, and Network Applications. *IEEE Commun. Surv. Tutor.* **2016**, *18*, 1413–1452. [CrossRef]
138. Otto, D. Induction Driven Vehicle: Pick-Up Coil Construction. New Zealand Patent 167422, 14 August 1974.
139. Bolger, J.G.; Ng, L.S.; Turner, D.B.; Wallace, R.I. Testing a Prototype Inductive Power Coupling for an Electric Highway System. In Proceedings of the 29th IEEE Vehicular Technology Conference, Arlington Heights, IL, USA, 27–30 March 1979; IEEE: New York, NY, USA; pp. 48–56.
140. Zell, C.E.; Bolger, J.G. Development of an engineering prototype of a roadway powered electric transit vehicle system: A public/private sector program. *IEEE Veh. Technol. Conf.* **1982**, 435–438.

141. Systems Control Technology, Inc. *Roadway Powered Electric Vehicle Project Track Construction and Testing Program Phase 3D*; University of California, Berkeley: Berkeley, CA, USA, 1994.
142. Shinohara, N. Wireless power transmission progress for electric vehicle in Japan. In Proceedings of the 2013 IEEE Radio and Wireless Symposium, Austin, TX, USA, 20–23 August 2013; pp. 109–111.
143. Sakamoto, H.; Harada, K.; Washimiya, S.; Takehara, K.; Matsuo, Y.; Nakao, F. Large air-gap coupler for inductive charger. *IEEE Trans. Magn.* **1999**, *35*, 3526–3528. [CrossRef]
144. Nikitin, P.; Rao, K.V.S.; Lazar, S. An overview of near field UHF RFID. In Proceedings of the 2007 IEEE International Conference on RFID, Grapevine, TX, USA, 26–28 March 2007; pp. 167–174.
145. Wireless Power Transfer—Electrical Engineering Stack Exchange. Power Supply—Is There Any Difference Between Induction and Resonant Wireless Energy Transfer—Electrical Engineering Stack Exchange. Available online: <https://electronics.stackexchange.com/questions/25176/isthere-any-difference-betweeninduction-and-resonant-wireless-energy-trans> (accessed on 8 August 2022).
146. Khan, S.; Ahmad, A.; Ahmad, F.; Shafaati Shemami, M.; Saad Alam, M.; Khateeb, S. A Comprehensive Review on Solar Powered Electric Vehicle Charging System. *Smart Sci.* **2018**, *6*, 54–79. [CrossRef]
147. Liang, J.; Wu, D.; Yu, J. A design method of compensation circuit for high-power dynamic capacitive power transfer system considering coupler voltage distribution for railway applications. *Electron* **2021**, *10*, 153. [CrossRef]
148. From Wireless to Dynamic Electric Vehicle Charging: The Evolution of Qualcomm Halo. Available online: <https://www.qualcomm.com/news/onq/2017/05/wireless-dynamic-ev-charging-evolution-qualcomm-halo> (accessed on 31 January 2023).
149. Mao, X.; Chen, J.; Zhang, Y.; Dong, J. A Simple and Reconfigurable Wireless Power Transfer System with Constant Voltage and Constant Current Charging. *IEEE Trans. Power Electron.* **2022**, *37*, 4921–4925. [CrossRef]
150. Kumar, R.; Bharj, R.S.; Bharj, J.; Singh, G.N.; Sharma, M. Solar-Based Electric Vehicle Charging Stations in India: A Perspective. *New Res. Dir. Sol. Energy Technol.* **2021**, 275–304.
151. Zhang, X.; Yuan, Z.; Yang, Q.; Li, Y.; Zhu, J.; Li, Y. Coil Design and Efficiency Analysis for Dynamic Wireless Charging System for Electric Vehicles. *IEEE Trans. Magn.* **2016**, *52*, 8700404. [CrossRef]
152. Jang, Y.J.; Jeong, S.; Lee, M.S. Initial energy logistics cost analysis for stationary, quasi-dynamic, & dynamic wireless charging public transportation systems. *Energies* **2016**, *9*, 483.
153. Zhang, Z.; Chau, K.T. Homogeneous Wireless Power Transfer for Move-and-Charge. *IEEE Trans. Power Electron.* **2015**, *30*, 6213–6220. [CrossRef]
154. Ko, Y.D.; Jang, Y.J. The optimal system design of the online electric vehicle utilizing wireless power transmission technology. *IEEE Trans. Intell. Transp. Syst.* **2013**, *14*, 1255–1265. [CrossRef]
155. Choi, S.Y.; Huh, J.; Lee, W.Y.; Rim, C.T. Asymmetric coil sets for wireless stationary EV chargers with large lateral tolerance by dominant field analysis. *IEEE Trans. Power Electron.* **2014**, *29*, 6406–6420. [CrossRef]
156. Choi, S.Y.; Jeong, S.Y.; Gu, B.W.; Lim, G.C.; Rim, C.T. Ultrathin S-Type Power Supply Rails for Roadway-Powered Electric Vehicles. *IEEE Trans. Power Electron.* **2015**, *30*, 6456–6468. [CrossRef]
157. ORNL Surges Forward with 20-Kilowatt Wireless Charging for Vehicles ORNL. Available online: <https://www.ornl.gov/news/ornl-surges-forward-20-kilowatt-wireless-charging-vehicles> (accessed on 12 August 2022).
158. Kim, J.H.; Lee, B.S.; Lee, J.H.; Lee, S.H.; Park, C.B.; Jung, S.M.; Lee, S.G.; Yi, K.P.; Baek, J. Development of 1-MW Inductive Power Transfer System for a High-Speed Train. *IEEE Trans. Ind. Electron.* **2015**, *62*, 6242–6250. [CrossRef]
159. Wu, H.H.; Masquelier, M.P. An overview of a 50-kW inductive charging system for electric buses. In Proceedings of the 2015 IEEE Transportation Electrification Conference and Expo (ITEC), Dearborn, MI, USA, 14–17 June 2015; pp. 1–4.
160. Taylor, M.F.; Blair Farley, K.; Gao, Y.; Bai, H.; Tse, Z.T.H. Electric vehicle wireless charging technology: A state-of-the-art review of magnetic coupling systems. *Wirel. Power Transf.* **2014**, *1*, 87–96.
161. Tritschler, J.; Reichert, S.; Goeldi, B. A practical investigation of a high power, bidirectional charging system for electric vehicles. In Proceedings of the 2014 16th European Conference on Power Electronics and Applications, Lappeenranta, Finland, 26–28 August 2014.
162. Li, W.; Zhao, H.; Li, S.; Deng, J.; Kan, T.; Mi, C.C. Integrated LCC Compensation Topology for Wireless Charger in Electric and Plug-in Electric Vehicles. *IEEE Trans. Ind. Electron.* **2015**, *62*, 4215–4225. [CrossRef]
163. Nguyen, T.D.; Li, S.; Li, W.; Mi, C.C. Feasibility study on bipolar pads for efficient wireless power chargers. In Proceedings of the 2014 IEEE Applied Power Electronics Conference and Exposition—APEC 2014, Fort Worth, TX, USA, 16–20 March 2014; pp. 1676–1682.
164. Lu, F.; Zhang, H.; Hofmann, H.; Mi, C. A high efficiency 3.3 kW loosely-coupled wireless power transfer system without magnetic material. In Proceedings of the 2015 IEEE Energy Conversion Congress and Exposition (ECCE), Montreal, QC, Canada, 20–24 September 2015; pp. 2282–2286.
165. Bojarski, M.; Asa, E.; Colak, K.; Czarkowski, D. A 25-kW industrial prototype wireless electric vehicle charger. In Proceedings of the 2016 IEEE Applied Power Electronics Conference and Exposition (APEC), Long Beach, CA, USA, 20–24 March 2016; pp. 1756–1761.
166. Bojarski, M.; Asa, E.; Colak, K.; Czarkowski, D. Analysis and control of multiphase inductively coupled resonant converter for wireless electric vehicle charger applications. *IEEE Trans. Transp. Electrification* **2017**, *3*, 312–320. [CrossRef]
167. Bosshard, R.; Kolar, J.W. Inductive Power Transfer for Electric Vehicle Charging: Technical challenges and tradeoffs. *IEEE Power Electron. Mag.* **2016**, *3*, 22–30. [CrossRef]

168. Li, S.; Mi, C.C. Wireless power transfer for electric vehicle applications. *IEEE J. Emerg. Sel. Top. Power Electron.* **2015**, *3*, 4–17.
169. Charging Electric Buses Quickly and Efficiently: Bus Stops Fitted with Modular Components Make 'Charge & Go' Simple to Implement. Available online: <http://www.conductix.us/en/news/2013-05-29/charging-electric-buses-quickly-and-efficiently-bus-stops-fitted-modular-components-make-charge-go> (accessed on 12 August 2022).
170. Wu, H.H.; Gilchrist, A.; Sealy, K.D.; Bronson, D. A high efficiency 5 kW inductive charger for EVs using dual side control. *IEEE Trans. Ind. Inform.* **2012**, *8*, 585–595. [CrossRef]
171. Sato, F.; Morita, J.; Takura, T.; Sato, T.; Matsuki, H. Research on Highly Efficient Contactless Power Station System using Meander Coil for Moving Electric Vehicle Model. *J. Magn. Soc. Japan* **2012**, *36*, 249–252. [CrossRef]
172. Chigira, M.; Nagatsuka, Y.; Kaneko, Y.; Abe, S.; Yasuda, T.; Suzuki, A. Small-size light-weight transformer with new core structure for contactless electric vehicle power transfer system. In Proceedings of the 2011 IEEE Energy Conversion Congress and Exposition, Phoenix, AZ, USA, 17–22 September 2011; pp. 260–266.
173. Budhia, M.; Covic, G.A.; Boys, J.T. Design and optimization of circular magnetic structures for lumped inductive power transfer systems. *IEEE Trans. Power Electron.* **2011**, *26*, 3096–3108. [CrossRef]
174. Kamineni, A.; Covic, G.A.; Boys, J.T. Analysis of Coplanar Intermediate Coil Structures in Inductive Power Transfer Systems. *IEEE Trans. Power Electron.* **2015**, *30*, 6141–6154. [CrossRef]
175. Bosshard, R.; Kolar, J.W.; Mühlethaler, J.; Stevanovic, I.; Wunsch, B.; Canales, F. Modeling and  $\eta$ - $\alpha$ -pareto optimization of inductive power transfer coils for electric vehicles. *IEEE J. Emerg. Sel. Top. Power Electron.* **2015**, *3*, 50–64. [CrossRef]
176. Horiuchi, T.; Kawashima, K. Study on Planar Antennas for Wireless Power Transmission of Electric Vehicles. *IEEJ Trans. Ind. Appl.* **2010**, *130*, 1371–1377. [CrossRef]
177. Van Schuylenbergh, K.; Puers, R. *Inductive Powering: Basic Theory and Application to Biomedical Systems*, 1st ed.; Springer: Dordrecht, The Netherlands, 2014.
178. Zhang, W.; Wong, S.C.; Tse, C.K.; Chen, Q. Analysis and comparison of secondary series-and parallel-compensated inductive power transfer systems operating for optimal efficiency and load-independent voltage-transfer ratio. *IEEE Trans. Power Electron.* **2014**, *29*, 2979–2990. [CrossRef]
179. Pinuela, M.; Yates, D.C.; Lucyszyn, S.; Mitcheson, P.D. Maximizing DC-to-load efficiency for inductive power transfer. *IEEE Trans. Power Electron.* **2013**, *28*, 2437–2447. [CrossRef]
180. Assawaworrarit, S.; Yu, X.; Fan, S. Robust wireless power transfer using a nonlinear parity-time-symmetric circuit. *Nature* **2017**, *546*, 387–390. [CrossRef] [PubMed]
181. Dong, Z.; Li, Z.; Yang, F.; Qiu, C.W.; Ho, J.S. Sensitive readout of implantable microsensors using a wireless system locked to an exceptional point. *Nat. Electron.* **2019**, *2*, 335–342. [CrossRef]
182. Schindler, J.; Li, A.; Zheng, M.C.; Ellis, F.M.; Kottos, T. Experimental study of active LRC circuits with PT symmetries. *Phys. Rev. A-At. Mol. Opt. Phys.* **2011**, *84*, 1–5. [CrossRef]
183. Zhou, J.; Zhang, B.; Xiao, W.; Qiu, D.; Chen, Y. Nonlinear Parity-Time-Symmetric Model for Constant Efficiency Wireless Power Transfer: Application to a Drone-in-Flight Wireless Charging Platform. *IEEE Trans. Ind. Electron.* **2019**, *66*, 4097–4107. [CrossRef]
184. Li, Y.; Hu, J.; Chen, F.; Li, Z.; He, Z.; Mai, R. Dual-phase-shift control scheme with current-stress and efficiency optimization for wireless power transfer systems. *IEEE Trans. Circuits Syst. I Regul. Pap.* **2018**, *65*, 3110–3121. [CrossRef]
185. Qiao, K.; Sun, P.; Rong, E.; Sun, J.; Zhou, H.; Wu, X. Anti-misalignment and lightweight magnetic coupler with H-shaped receiver structure for AUV wireless power transfer. *IET Power Electron.* **2022**, *15*, 1843–1857. [CrossRef]
186. Liu, H.; Li, Z.; Tian, Y.; Liu, Y.; Song, W. Anti-misalignment capability optimization for laminated magnetic couplers in wireless charging systems using balanced particle swarm optimization method. *J. Power Electron.* **2022**, *23*, 345–354. [CrossRef]
187. Wu, M.; Yang, X.; Chen, W.; Wang, L.; Jiang, Y.; Gao, Q.; Yu, X. A Compact Coupler with Integrated Multiple Decoupled Coils for Wireless Power Transfer System and Its Anti-misalignment Control. *IEEE Trans. Power Electron.* **2022**, *37*, 12814–12827. [CrossRef]
188. Li, J.; Yin, F.; Wang, L.; Cui, B.; Yang, D. Electromagnetic induction position sensor applied to anti-misalignment wireless charging for UAVs. *IEEE Sens. J.* **2019**, *20*, 515–524. [CrossRef]
189. Buja, G.; Bertoluzzo, M.; Dashora, H.K. Lumped Track Layout Design for Dynamic Wireless Charging of Electric Vehicles. *IEEE Trans. Ind. Electron.* **2016**, *63*, 6631–6640. [CrossRef]
190. Ahmad, A.; Alam, M.S.; Chabaan, R. A Comprehensive Review of Wireless Charging Technologies for Electric Vehicles. *IEEE Trans. Transp. Electrif.* **2017**, *4*, 38–63. [CrossRef]
191. Kim, B.H.C.; Seo, D.H.; You, J.S.; Park, J.H.; Cho, B.H. Design of a contactless battery charger for cellular phone. *IEEE Trans. Ind. Electron.* **2001**, *48*, 1238–1247.
192. Redder, D.A.G.; Brown, A.D.; Andrew Skinner, J. A contactless electrical energy transmission system. *IEEE Trans. Ind. Electron.* **1999**, *46*, 23–30.
193. Valtchev, S.; Borges, B.; Brandisky, K.; Ben Klaassens, J. Resonant contactless energy transfer with improved efficiency. *IEEE Trans. Power Electron.* **2009**, *24*, 685–699. [CrossRef]
194. Hwang, K.; Cho, J.; Kim, D.; Park, J.; Kwon, J.H.; Kwak, S.I.; Park, H.H.; Ahn, S. An Autonomous Coil Alignment System for the Dynamic Wireless Charging of Electric Vehicles to Minimize Lateral Misalignment. *Energies* **2017**, *10*, 315. [CrossRef]
195. Liu, N.; Habetler, T.G. Design of a Universal Inductive Charger for Multiple Electric Vehicle Models. *IEEE Trans. Power Electron.* **2015**, *30*, 6378–6390. [CrossRef]

196. Villa, J.L.; Sallan, J.; Sanz Osorio, J.F.; Llombart, A. High-misalignment tolerant compensation topology for ICPT systems. *IEEE Trans. Ind. Electron.* **2012**, *59*, 945–951. [[CrossRef](#)]
197. Kim, S.; Covic, G.A.; Boys, J.T. Tripolar pad for inductive power transfer systems for EV charging. *IEEE Trans. Power Electron.* **2017**, *32*, 5045–5057. [[CrossRef](#)]
198. Zhang, Y.; Zhao, Z.; Chen, K. Frequency decrease analysis of resonant wireless power transfer. *IEEE Trans. Power Electron.* **2014**, *29*, 1058–1063. [[CrossRef](#)]
199. Kim, S.; Covic, G.A.; Boys, J.T. Analysis on Tripolar Pad for Inductive Power Transfer systems. In Proceedings of the 2016 IEEE PELS Workshop on Emerging Technologies: Wireless Power Transfer (WoW), Knoxville, TN, USA, 4–6 October 2016; pp. 15–20.
200. International Commission on Non-Ionizing Radiation Protection. Guidelines for limiting exposure to time-varying electric and magnetic fields (1 Hz to 100 kHz). *Health Phys.* **2010**, *99*, 818–836. [[CrossRef](#)] [[PubMed](#)]
201. Miller, J.M.; Daga, A. Elements of Wireless Power Transfer Essential to High Power Charging of Heavy-Duty Vehicles. *IEEE Trans. Transp. Electrification.* **2015**, *1*, 26–39. [[CrossRef](#)]
202. Zaheer, A.; Covic, G.A.; Kacprzak, D. A bipolar pad in a 10-kHz 300-W distributed IPT system for AGV applications. *IEEE Trans. Ind. Electron.* **2014**, *61*, 3288–3301. [[CrossRef](#)]
203. Covic, G.A.; Kissin, M.L.G.; Kacprzak, D.; Clausen, N.; Hao, H. A bipolar primary pad topology for EV stationary charging and highway power by inductive coupling. In Proceedings of the IEEE Energy Conversion Congress and Exposition, Phoenix, AZ, USA, 17–22 September 2011; pp. 1832–1838.
204. Electric Vehicle (EV) Charging Infrastructure Services. Available online: <https://www.ul.com/services/electric-vehicle-ev-charging-infrastructure-services> (accessed on 10 September 2022).
205. Bi, Z.; Kan, T.; Mi, C.C.; Zhang, Y.; Zhao, Z.; Keoleian, G.A. A review of wireless power transfer for electric vehicles: Prospects to enhance sustainable mobility. *Appl. Energy.* **2016**, *179*, 413–425. [[CrossRef](#)]
206. Jeong, S.; Jang, Y.J.; Kum, D. Economic Analysis of the Dynamic Charging Electric Vehicle. *IEEE Trans. Power Electron.* **2015**, *30*, 6368–6377. [[CrossRef](#)]
207. Wei, X.; Wang, Z.; Dai, H. A Critical Review of Wireless Power Transfer via Strongly Coupled Magnetic Resonances. *Energies* **2014**, *7*, 4316–4341. [[CrossRef](#)]
208. Byeong-Mun, S.; Kratz, R.; Gurol, S. Contactless inductive power pickup system for Maglev applications. In Proceedings of the Conference Record of the 2002 IEEE Industry Applications Conference, 37th IAS Annual Meeting (Cat. No.02CH37344), Pittsburgh, PA, USA, 13–18 October 2002; Volume 3, pp. 1586–1591.
209. Lee, W.Y.; Huh, J.; Choi, S.Y.; Thai, X.V.; Kim, J.H.; Al-Amman, E.A.; Rim, C.T. Finite-Width Magnetic Mirror Models of Mono and Dual Coils for Wireless Electric Vehicles. *IEEE Trans. Power Electron.* **2013**, *28*, 1413–1428. [[CrossRef](#)]
210. Huh, J.; Lee, W.; Lee, W.Y.; Cho, G.H.; Rim, C.T. Narrow-Width Inductive Power Transfer System for Online Electrical Vehicles. *IEEE Trans. Power Electron.* **2011**, *26*, 3666–3679. [[CrossRef](#)]
211. Covic, G.A.; Boys, J.T. Modern trends in inductive power transfer for transportation applications. *IEEE J. Emerg. Sel. Top. Power Electron.* **2013**, *1*, 28–41. [[CrossRef](#)]
212. Sabanci, K.; Balci, S.; Aslan, M.F. An ensemble learning estimation of the effect of magnetic coupling on switching frequency value in wireless power transfer system for electric vehicles. *SN Appl. Sci.* **2019**, *1*, 1712. [[CrossRef](#)]
213. Okasili, I.; Elkhateb, A.; Littler, T. A Review of Wireless Power Transfer Systems for Electric Vehicle Battery Charging with a Focus on Inductive Coupling. *Electronics* **2022**, *11*, 1355. [[CrossRef](#)]
214. Nguyen, H.T.; Alsawalhi, J.Y.; Al Hosani, K.; Al-Sumaiti, A.S.; Al Jaafari, K.A.; Byon, Y.J.; El Moursi, M.S. Review map of comparative designs for wireless high-power transfer systems in EV applications: Maximum efficiency, ZPA, and CC/CV modes at fixed resonance frequency independent from coupling coefficient. *IEEE Trans. Power Electron.* **2021**, *37*, 4857–4876. [[CrossRef](#)]
215. Li, L.; Wang, Z.; Gao, F.; Wang, S.; Deng, J. A family of compensation topologies for capacitive power transfer converters for wireless electric vehicle charger. *Appl. Energy* **2020**, *260*, 114156. [[CrossRef](#)]
216. Long, B.R.; Miller, J.M.; Daga, A.; Schrafel, P.C.; Wolgemuth, J. Which way for wireless power: High Q or high k? In Proceedings of the 2016 IEEE PELS Workshop on Emerging Technologies: Wireless Power Transfer (WoW), Knoxville, TN, USA, 4–6 October 2016; pp. 6–10.
217. Elliott, G.A.J.; Raabe, S.; Covic, G.A.; Boys, J.T. Multiphase pickups for large lateral tolerance contactless power-transfer systems. *IEEE Trans. Ind. Electron.* **2010**, *57*, 1590–1598. [[CrossRef](#)]
218. Patil, D.; Ditsworth, M.; Pacheco, J.; Cai, W. A magnetically enhanced wireless power transfer system for compensation of misalignment in mobile charging platforms. In Proceedings of the 2015 IEEE Energy Conversion Congress and Exposition (ECCE), Montreal, QC, Canada, 20–24 September 2015; pp. 1286–1293.
219. Boys, J.T.; Covic, G.A. IPT Fact Sheet Series: No.2 Magnetic Circuits for Powering Electric Vehicles. Department of Electrical and Computer Engineering, The University of Auckland: Auckland, New Zealand, 2014.
220. Ni, W.; Collings, I.B.; Wang, X.; Liu, R.P.; Kajan, A.; Hedley, M.; Abolhasan, M. Radio alignment for inductive charging of electric vehicles. *IEEE Trans. Ind. Inform.* **2015**, *11*, 427–440. [[CrossRef](#)]
221. Shevchenko, V.; Husev, O.; Strzelecki, R.; Pakhaliuk, B.; Poliakov, N.; Strzelecka, N. Compensation topologies in IPT systems: Standards, requirements, classification, analysis, comparison and application. *IEEE Access* **2019**, *7*, 120559–120580. [[CrossRef](#)]
222. Zhang, W.; Mi, C.C. Compensation topologies of high-power wireless power transfer systems. *IEEE Trans. Veh. Technol.* **2016**, *65*, 4768–4778. [[CrossRef](#)]

223. Cho, J.-H.; Lee, B.-H.; Kim, Y.-J. Maximizing Transfer Efficiency with an Adaptive Wireless Power Transfer System for Variable Load Applications. *Energies* **2021**, *14*, 1417. [\[CrossRef\]](#)
224. Pantic, Z.; Bai, S.; Lukic, S.M. ZCS LCC-compensated resonant inverter for inductive-power-transfer application. *IEEE Trans. Ind. Electron.* **2011**, *58*, 3500–3510. [\[CrossRef\]](#)
225. Hsieh, Y.C.; Lin, Z.R.; Chen, M.C.; Hsieh, H.C.; Liu, Y.C.; Chiu, H.J. High-Efficiency Wireless Power Transfer System for Electric Vehicle Applications. *IEEE Trans. Circuits Syst. II Express Briefs* **2017**, *64*, 942–946. [\[CrossRef\]](#)
226. Cheng, L.; Ki, W.H.; Lu, Y.; Yim, T.S. Adaptive On/Off Delay-Compensated Active Rectifiers for Wireless Power Transfer Systems. *IEEE J. Solid-State Circuits* **2016**, *51*, 712–723.
227. Zhang, W.; White, J.C.; Malhan, R.K.; Mi, C.C. Loosely Coupled Transformer Coil Design to Minimize EMF Radiation in Concerned Areas. *IEEE Trans. Veh. Technol.* **2016**, *65*, 4779–4789. [\[CrossRef\]](#)
228. Li, W.; Zhao, H.; Deng, J.; Li, S.; Mi, C.C. Comparison Study on SS and double-sided LCC compensation topologies for EV/PHEV Wireless Chargers. *IEEE Trans. Veh. Technol.* **2016**, *65*, 4429–4439. [\[CrossRef\]](#)
229. Lee, S.H.; Lee, B.S.; Lee, J.H. A new design methodology for a 300-kW, low flux density, large air gap, online wireless power transfer system. *IEEE Trans. Ind. Appl.* **2016**, *52*, 4234–4242. [\[CrossRef\]](#)
230. Jegadeesan, R.; Guo, Y.X. Topology selection and efficiency improvement of inductive power links. *IEEE Trans. Antennas Propag.* **2012**, *60*, 4846–4854. [\[CrossRef\]](#)
231. Hariri, A.O.; Youssef, T.; Elsayed, A.; Mohammed, O. A Computational Approach for a Wireless Power Transfer Link Design Optimization Considering Electromagnetic Compatibility. *IEEE Trans. Magn.* **2016**, *52*, 1–4. [\[CrossRef\]](#)
232. Liu, F.; Yang, Y.; Jiang, D.; Ruan, X.; Chen, X. Modeling and optimization of magnetically coupled resonant wireless power transfer system with varying spatial scales. *IEEE Trans. Power Electron.* **2017**, *32*, 3240–3250. [\[CrossRef\]](#)
233. Abou Houran, M.; Yang, X.; Chen, W. Magnetically Coupled Resonance WPT: Review of Compensation Topologies, Resonator Structures with Misalignment, and EMI Diagnostics. *Electronics* **2018**, *7*, 296. [\[CrossRef\]](#)
234. Hirai, J.; Kim, T.W.; Kawamura, A. Study on intelligent battery charging using inductive transmission of power and information. *IEEE Trans. Power Electron.* **2000**, *15*, 335–345. [\[CrossRef\]](#)
235. Liu, F.; Zhang, Y.; Chen, K.; Zhao, Z.; Yuan, L. A comparative study of load characteristics of resonance types in wireless transmission systems. In Proceedings of the 2016 Asia-Pacific International Symposium on Electromagnetic Compatibility (APEMC), Shenzhen, China, 17–21 May 2016; pp. 203–206.
236. Wang, Y.; Yao, Y.; Liu, X.; Xu, D. S/CLC compensation topology analysis and circular coil design for wireless power transfer. *IEEE Trans. Transp. Electrification* **2017**, *3*, 496–507. [\[CrossRef\]](#)
237. Samanta, S.; Rathore, A.K. A New Current-Fed CLC Transmitter and LC Receiver Topology for Inductive Wireless Power Transfer Application: Analysis, Design, and Experimental Results. *IEEE Trans. Transp. Electrification* **2015**, *1*, 357–368. [\[CrossRef\]](#)
238. Feng, H.; Cai, T.; Duan, S.; Zhao, J.; Zhang, X.; Chen, C. An LCC-Compensated Resonant Converter Optimized for Robust Reaction to Large Coupling Variation in Dynamic Wireless Power Transfer. *IEEE Trans. Ind. Electron.* **2016**, *63*, 6591–6601. [\[CrossRef\]](#)
239. Li, S.; Li, W.; Deng, J.; Nguyen, T.D.; Mi, C.C. A Double-Sided LCC Compensation Network and Its Tuning Method for Wireless Power Transfer. *IEEE Trans. Veh. Technol.* **2015**, *64*, 2261–2273. [\[CrossRef\]](#)
240. Chen, Y.; Zhang, H.; Park, S.-J.; Kim, D.-H. A Comparative Study of S-S and LCCL-S Compensation Topologies in Inductive Power Transfer Systems for Electric Vehicles. *Energies* **2019**, *12*, 1913. [\[CrossRef\]](#)
241. Deng, J.; Li, W.; Nguyen, T.D.; Li, S.; Mi, C.C. Compact and Efficient Bipolar Coupler for Wireless Power Chargers: Design and Analysis. *IEEE Trans. Power Electron.* **2015**, *30*, 6130–6140. [\[CrossRef\]](#)
242. Kan, T.; Nguyen, T.D.; White, J.C.; Malhan, R.K.; Mi, C.C. A new integration method for an electric vehicle wireless charging system using LCC compensation topology: Analysis and design. *IEEE Trans. Power Electron.* **2017**, *7*, 1638–1650. [\[CrossRef\]](#)
243. Lu, F.; Zhang, H.; Hofmann, H.; Mi, C.C. A Dynamic Charging System with Reduced Output Power Pulsation for Electric Vehicles. *IEEE Trans. Ind. Electron.* **2016**, *63*, 6580–6590. [\[CrossRef\]](#)
244. Park, M.; Nguyen, V.T.; Yu, S.D.; Yim, S.W.; Park, K.; Min, B.D.; Do Kim, S.; Cho, J.G. A study of wireless power transfer topologies for 3.3 kW and 6.6 kW electric vehicle charging infrastructure. In Proceedings of the 2016 IEEE Transportation Electrification Conference and Expo, Asia-Pacific (ITEC Asia-Pacific), Busan, Republic of Korea, 1–4 June 2016; pp. 689–692.
245. Campi, T.; Cruciani, S.; Maradei, F.; Feliziani, M. Near-Field Reduction in a Wireless Power Transfer System Using LCC Compensation. *IEEE Trans. Electromagn. Compat.* **2017**, *59*, 686–694. [\[CrossRef\]](#)
246. Zaheer, A.; Neath, M.; Beh, H.Z.; Covic, G.A. A dynamic EV charging system for slow moving traffic applications. *IEEE Trans. Transp. Electrification* **2017**, *3*, 354–369. [\[CrossRef\]](#)
247. Cirimele, V.; Freschi, F.; Guglielmi, P. Wireless power transfer structure design for electric vehicle in charge while driving. In Proceedings of the 2014 International Conference on Electrical Machines (ICEM), Berlin, Germany, 2–5 September 2014; pp. 2461–2467.
248. Onar, O.C.; Miller, J.M.; Campbell, S.L.; Coomer, C.; White, C.P.; Seiber, L.E. A novel wireless power transfer for in-motion EV/PHEV charging. In Proceedings of the 2013 Twenty-Eighth Annual IEEE Applied Power Electronics Conference and Exposition (APEC), Long Beach, CA, USA, 17–21 March 2013; pp. 3073–3080.

249. Cirimele, V.; Pichon, L.; Freschi, F. Electromagnetic modeling and performance comparison of different pad-to-pad length ratio for dynamic inductive power transfer. In Proceedings of the IECON 2016—42nd Annual Conference of the IEEE Industrial Electronics Society, Florence, Italy, 23–26 October 2016; pp. 4499–4503.
250. Campi, T.; Cruciani, S.; De Santis, V.; Feliziani, M. EMF safety and thermal aspects in a pacemaker equipped with a wireless power transfer system working at low frequency. *IEEE Trans. Microw. Theory Tech.* **2016**, *64*, 375–382. [CrossRef]
251. Fang, W.; Deng, H.; Liu, Q.; Liu, M.; Jiang, Q.; Yang, L.; Giannakis, G.B. Safety Analysis of Long-Range and High-Power Wireless Power Transfer Using Resonant Beam. *IEEE Trans. Signal Process.* **2021**, *69*, 2833–2843. [CrossRef]
252. Dai, R.; Zhao, Y.; Chen, G.; Dou, W.; Tian, C.; Wu, X.; He, T. Robustly Safe Charging for Wireless Power Transfer. In Proceedings of the IEEE INFOCOM 2018—IEEE Conference on Computer Communications, Honolulu, HI, USA, 16–19 April 2018; pp. 378–386.
253. Giler, E. WiTricity. Available online: [https://www.ted.com/talks/eric\\_giler\\_demos\\_wireless\\_electricity](https://www.ted.com/talks/eric_giler_demos_wireless_electricity) (accessed on 20 August 2022).
254. Zhang, W.; Xia, L.; Hong, X.; Gong, C.; Shen, L.; Ruan, Z.; Negue, D.M. Comparison of Compensation Topologies for Wireless Charging Systems in EV Applications. In Proceedings of the 2022 International Conference on Artificial Intelligence in Everything (AIE), Lefkosa, Cyprus, 2–4 August 2022; pp. 17–22.
255. Moon, H.; Kim, S.; Park, H.H.; Ahn, S. Design of a resonant reactive shield with double coils and a phase shifter for wireless charging of electric vehicles. *IEEE Trans. Magn.* **2015**, *51*, 18–21.
256. Monti, G.; Masotti, D.; Paolini, G.; Corchia, L.; Costanzo, A.; Dionigi, M.; Mastri, F.; Mongiardo, M.; Sorrentino, R.; Tarricone, L. EMC and EMI issues of WPT systems for wearable and implantable devices. *IEEE Electromagn. Compat. Mag.* **2018**, *7*, 67–77. [CrossRef]
257. Lu, M.H.; Jen, M.U. Safety design of electric vehicle charging equipment. *World Electr. Veh. J.* **2012**, *5*, 1017–1024. [CrossRef]
258. IEC Webstore. Standard IEC 61980-1:2015. Available online: <https://webstore.iec.ch/publication/22951> (accessed on 23 August 2022).
259. IEC Webstore. Standard IEC 61980-1:2020. Available online: <https://webstore.iec.ch/publication/31657> (accessed on 23 August 2022).
260. Electric Vehicle Wireless Power Transfer (WPT) Systems—Part 1: General Requirements, IEC 61980-1:2015/COR1:2017. Available online: <https://webstore.iec.ch/publication/59640> (accessed on 23 August 2022).
261. IEC—TC 69 Dashboard &GT. Documents: Working Documents, Other Documents, Support Documents. Available online: [https://www.iec.ch/ords/f?p=103:30:1475872635832:::FSP\\_ORG\\_ID,FSP\\_LANG\\_ID:1255,25](https://www.iec.ch/ords/f?p=103:30:1475872635832:::FSP_ORG_ID,FSP_LANG_ID:1255,25) (accessed on 24 August 2022).
262. IEEE Standard for Safety Levels with Respect to Human Exposure to Electric, Magnetic, and Electromagnetic Fields, 0 Hz to 300 GHz. Available online: <https://standards.ieee.org/ieee/C95.1/4940/> (accessed on 24 August 2022).
263. Wireless Power Transfer for Light-Duty Plug-In/Electric Vehicles and Alignment Methodology—SAE International. Available online: [https://www.sae.org/standards/content/j2954\\_202208/](https://www.sae.org/standards/content/j2954_202208/) (accessed on 24 August 2022).
264. SAE Electric Vehicle Inductively Coupled Charging—SAE International. Available online: [http://standards.sae.org/j1773\\_2014\\_06/](http://standards.sae.org/j1773_2014_06/) (accessed on 24 August 2022).
265. Communication between Wireless Charged Vehicles and Wireless EV Chargers. *SAE International*. Available online: [http://standards.sae.org/j2847/6\\_201508/](http://standards.sae.org/j2847/6_201508/) (accessed on 10 September 2022).
266. Signaling Communication for Wirelessly Charged Electric Vehicles—SAE International. Available online: [http://standards.sae.org/j2931/6\\_201508/](http://standards.sae.org/j2931/6_201508/) (accessed on 10 September 2022).
267. Wang, Z.; Cui, S.; Han, S.; Song, K.; Zhu, C.; Matveevich, M.I.; Yurievich, O.S. A Novel Magnetic Coupling Mechanism for Dynamic Wireless Charging System for Electric Vehicles. *IEEE Trans. Veh. Technol.* **2018**, *67*, 124–133. [CrossRef]
268. Available online: [www.pluglesspower.com](http://www.pluglesspower.com) (accessed on 26 January 2023).
269. IEC 61851-1; Electric Vehicle Conductive Charging System—Part 1: General Requirements. IEC (International Electrotechnical Commission): Geneva, Switzerland, 2010.
270. Italian Regulatory Authority for Electricity Gas and Water. Available online: [www.autorita.energia.it](http://www.autorita.energia.it) (accessed on 26 January 2023).

**Disclaimer/Publisher’s Note:** The statements, opinions and data contained in all publications are solely those of the individual author(s) and contributor(s) and not of MDPI and/or the editor(s). MDPI and/or the editor(s) disclaim responsibility for any injury to people or property resulting from any ideas, methods, instructions or products referred to in the content.